NOVA SCHOOL OF SCIENCE & TECHNOLOGY

DEPARTMENT OF PHYSICS

INÊS MORAIS LUDOVINO

BSc in Biomedical Engineering

DEVELOPMENT OF A TRANSHUMERAL PROSTHESIS WITH FLEXIBLE MATERIALS BY 3D PRINTING

MASTER IN BIOMEDICAL ENGINEERING

NOVA University Lisbon
September, 2024

NOVA SCHOOL OF
SCIENCE & TECHNOLOGY

DEPARTMENT OF
PHYSICS

DEVELOPMENT OF A TRANSHUMERAL PROSTHESIS WITH FLEXIBLE MATERIALS BY 3D PRINTING

INÊS MORAIS LUDOVINO

BSc in Biomedical Engineering

Adviser: Bruno Alexandre Rodrigues Simões Soares
Assistant Professor, NOVA SST

Co-adviser: Cláudia Regina Pereira Quaresma
Assistant Professor, NOVA SST

Examination Committee

Chair: Hugo Filipe Silveira Gamboa
Full Professor, NOVA SST

Rapporteur: Jorge Alexandre Monteiro de Carvalho e Silva
Associate Professor, NOVA SST

Adviser: Bruno Alexandre Rodrigues Simões Soares
Assistant Professor, NOVA SST

MASTER IN BIOMEDICAL ENGINEERING

NOVA University Lisbon
September, 2024

Development of a transhumeral prosthesis with flexible materials by 3D printing

This document was created with the (pdf/Xe/Lua)LaTeX processor and the NOVAthesis template (v7.1.5) [1].

Para a minha família,

Acknowledgements

A realização deste projeto foi uma das experiências mais gratificantes que já tive e fico muito feliz por ter feito a escolha certa no que diz respeito ao tema, que tanto me fascina e me deu gozo desenvolver, e ao curso em si, Engenharia Biomédica. Por outro lado, foi também desafiador em muitos níveis e tenho a certeza que não teria sido possível concluí-lo sem o apoio que recebi.

Em primeiro lugar, gostaria de agradecer ao meu orientador, Bruno Soares, pelas inúmeras ideias, pela sabedoria partilhada, pela ajuda e pela calma que me transmitiu ao longo destes meses. À minha co-orientadora, Cláudia Quaresma, gostaria de agradecer pelo apoio incansável e por ter tornado tudo possível.

Agradeço ao Departamento de Física (DF) e ao Departamento de Engenharia Mecânica e Industrial (DEMI) da Faculdade de Ciências e Tecnologia da Universidade Nova de Lisboa, pela disponibilização das instalações e equipamentos, permitindo-me trabalhar ao lado de colegas sempre dispostos a ajudar. Ao Hospital Dona Estefânia, especialmente à terapeuta Alexandra Quintas, agradeço por se ter disponibilizado a colaborar e me ter proporcionado uma visão clínica valiosa da temática que o projeto aborda.

À Ana Oliveira, um obrigada especial pela ajuda preciosa e por todas as dicas, que não só foram úteis agora, mas que, sem dúvida, continuarão a ser no futuro.

Ao Tiago, a melhor pessoa que podia ter ao meu lado, obrigada pelos conselhos, pela ajuda e, sobretudo, pela paciência infinita.

À Margarida, a minha verdadeira companheira de curso/vida, obrigada por teres acompanhado esta fase, assim como todas as outras até agora, e por me compreenderes como ninguém.

À Carolina P., Carolina J., Teresa, Laura, Daniela, Mafalda, Inês e Joana, as melhores amigas que podia ter, obrigada pelo vosso apoio, foi muito importante para chegar até aqui. Aos restantes amigos incríveis que a FCT me deu, obrigada.

À minha família, obrigada por tudo. Aos melhores pais do mundo, que tiveram um papel fundamental em muitas partes deste trabalho, esta dissertação também é um bocadinho vossa. Espero que o fim deste percurso, que vocês tornaram possível, vos deixe orgulhosos e seja recompensador de todos os esforços que fizeram e de todas as respostas

tortas que levaram. À minha avó, que ajudou no que podia. Aos meus tios, primos e madrinha, que sempre me apoiaram. Aos meus avós e avô, que olham por mim de longe. E, claro, ao meu Sparky.

A todos, o meu mais sincero obrigada.

Abstract

Currently, several prosthetic solutions are produced using Additive Manufacturing (AM), such as the e-NABLE prostheses. However, despite low cost, these prostheses are often uncomfortable, less functional, and aesthetically unpleasing. This work aims to redesign an existent e-NABLE prosthesis and develop a body-powered transhumeral device that is functional and anthropomorphic, combining rigid and flexible materials for improved comfort.

The first stage involved studying a specific clinical case, an eight-year-old girl with a transhumeral amputation. This included understanding her needs and assessing her upper limbs anatomy, through measurements and Three-dimensional (3D) scanning. To develop a comprehensive device, testimonies from other children with similar conditions and healthcare professionals were also gathered. The next stage focused on the prosthesis design, with the creation of several prototypes, using Computer-Aided Design (CAD) software and 3D printing, until the desired model was achieved. The final prototype was assembled and several tests were performed to assess its performance and resistance. Additionally, Finite Element Analysis (FEA) was performed to simulate force application and study the device's behavior. An ongoing study was conducted to find the most suitable materials, focusing on achieving comfort without losing functionality. Finally, the prosthesis was presented to the child for evaluation.

This project resulted in a prosthesis that weighs 400 g and combines affordability, comfort, aesthetics and functionality, despite some limitations. The device incorporates flexible materials and an anthropomorphic design, enabling the terminal device to fully close, requiring between 85.3 N and 163.2 N of force, powered by the amputee's shoulder movements. It also performs shoulder internal/external rotation, elbow flexion/extension and forearm supination/pronation. However, while it can hold loads up to at least 0.9 kg, its inability to maintain a grip remains a challenge. Moreover, it is applicable to other individuals with transhumeral deficiencies.

Keywords: Additive Manufacturing, Flexible Materials, Transhumeral Prostheses, Body-powered Prostheses

Resumo

Atualmente, existe uma ampla variedade de próteses produzidas por Fabrico Aditivo como, por exemplo, as próteses e-NABLE. Apesar dos seus baixos custos, estas próteses revelam-se por vezes desconfortáveis, pouco funcionais e esteticamente pouco atraentes. O objetivo do presente trabalho foi desenvolver uma prótese transhumeral *body-powered*, que fosse funcional, antropomórfica e que combinasse materiais rígidos e flexíveis para um maior conforto, tendo por base uma prótese e-NABLE já existente.

A primeira etapa deste trabalho envolveu o estudo de um caso clínico especifico: uma criança de oito anos com uma amputação transumeral. Tal inclui a compreensão das necessidades da criança, bem como uma avaliação da anatomia dos seus membros superiores, realizada através de medições e *scanning* 3D. De forma a desenvolver um dispositivo abrangente, foram também recolhidos testemunhos de outras criaças com condições semelhantes e de profissionais de saúde. A etapa seguinte centrou-se no *design* da prótese, com a criação de vários protótipos, utilizando *software* CAD e impressão 3D, até se alcançar o modelo desejado. O protótipo final foi submetido a diversos testes para avaliar o seu desempenho e resistência e ainda a uma Análise de Elementos Finitos (FEA), para simular a aplicação de forças e estudar o comportamento do dispositivo. Paralelamente, foi realizado um estudo para identificar os melhores materiais para o dispositivo, com foco em garantir conforto sem comprometer funcionalidade. Por fim, a prótese foi apresentada à criança para avaliação.

Este projeto resultou numa prótese de 400 g que combina baixo custo, conforto, estética e funcionalidade, embora tenha algumas limitações. O dispositivo incorpora materiais flexíveis, um *design* antropomórfico e permite a flexão completa dos dedos da mão, o que requer uma força compreendida entre 85.3 N e 163.2 N, acionada por movimentos do ombro do amputado. Realiza também movimentos de rotação interna/externa do ombro, flexão/extensão do cotovelo e supinação/pronação do antebraço. No entanto, apesar de conseguir suportar cargas até, pelo menos, 0.9 kg, manter um *grip* constante continua um desafio. A prótese desenvolvida pode também ser aplicada a outras pessoas com amputação transumeral.

Palavras-chave: Fabrico Aditivo, Materiais Flexíveis, Próteses Transumerais, Próteses *body-powered*

Contents

List of Figures

List of Tables

Acronyms

2D Two-dimensional *(pp. 6, 10, 26)*
3D Three-dimensional *(pp. v, 1, 6, 7, 10, 12, 14–16, 19–21, 23, 26–28, 37–40, 53)*

ABS Acrylonitrile Butadiene Styrene *(pp. 6, 7, 14)*
AM Additive Manufacturing *(pp. v, 3, 6, 14)*
ASA Acrylonitrile styrene acrylate *(p. 6)*

CAD Computer-Aided Design *(pp. v, 6, 19)*
CMC carpometacarpal *(pp. 3, 24, 34, 39)*

DOFs Degrees of Freedom *(pp. 4, 11, 12, 14, 38, 39)*

EEG electroencefalography *(p. 8)*
EMG electromyography *(p. 8)*

FDM Fused Deposition Modeling *(pp. 6, 7)*
FEA Finite Element Analysis *(pp. v, x, xi, 14, 15, 24, 28, 35, 40, 55, 61, 65)*
FEM Finit Element Method *(pp. 24, 38, 62)*
FOS Factor of Safety *(pp. 25, 36)*

MP metacarpophalangeal *(pp. 3, 24, 34, 39)*

NIOP No-Insurance Optimized Prostheses *(p. 12)*

PETG Polyethylene Terephthalate Glycol *(pp. 6, 7, 28, 37)*
PLA Polylactic Acid *(pp. 6, 7, 13, 14, 17, 20, 21, 25, 28, 29)*
PVA Polyvinyl Alcohol *(p. 14)*

SD Standard Deviation *(p. 24)*

STL Standard Tessellation Language *(pp. 6, 16, 19)*

TPE Thermoplastic Elastomers *(pp. 6, 7)*
TPU Thermoplastic Polyurethane *(pp. 6, 7, 20, 21, 24, 25, 28, 29, 35–37)*

VC Voluntary Closing *(pp. 10, 11, 14, 32, 39)*
VO Voluntary opening *(p. 10)*

1 Introduction

In this chapter, the motivations behind this study and its main objectives are explained. Transhumeral disabilities, whether acquired or congenital, have a significant impact on people's quality of life and prosthetic rehabilitation can help overcome the adversities caused by the absence of an upper limb. Although a wide range of prosthetic options are currently available to meet the diverse needs of patients, the high rejection rates associated with their use represent a significant concern.

1.1 Motivation

The main motivation for this work is the reduction of the high rejection rates associated with wearing prosthetics, stemming from different factors. Addressing this issue is crucial, considering the promising potential of prosthetics to significantly improve the lives of individuals with limb deficiencies.

Currently, in the market, there is a scarcity of options for transhumeral amputees, and only a few of them manage to combine affordability, functionality, comfort, and aesthetics. Therefore, this work aims to develop a solution that addresses all these aspects, in order to help reduce rejection rates, improving not only the life of the case-study child, but also of other children facing similar upper limb disabilities.

1.2 Study Goals

The main goal of this work is to develop a 3D printed body-powered transhumeral prosthesis for individuals with transhumeral amputations. This project was specifically based on the case of an eight-year-old child with a congenital deficiency in the left upper limb. Furthermore, it may serve the needs of other transhumeral amputees in the future.

A prosthesis named *NIOP TH-S* [2], presented in Section 3.1, is the starting point of this work. The goal is to redesign this prosthesis to address identified functional issues, incorporate flexible materials, and improve aesthetics to better fit the needs of the case-study child. The redesigned prosthesis aims to be lightweight and functional, combining

rigid and flexible materials to enhance comfort, and aims to have an anthropomorphic design that closely matches the unaffected limb in terms of skin tone, size, and shape.

These considerations not only contribute to the physical well-being of the amputees, who face daily challenges due to their reduced physical capabilities, but also aim to address social challenges associated with wearing prosthetics. These challenges include feelings such as shame, low self-esteem and social isolation, which can exacerbate psychological concerns [3].

By pursuing these objectives, this work aims to reduce the high rejection rates associated with this type of prostheses, particularly in children, which is the primary focus of this work.

1.3 Document Organization

This work is organized into six main chapters:

- **Chapter 1 - Introduction:** provides the background, context and the goals of this study.
- **Chapter 2 - Theoretical Concepts:** presents the concepts that are relevant to this work.
- **Chapter 3 - State Of The Art:** reviews existing prosthetic solutions and analyses their limitations.
- **Chapter 4 - Methodology:** describes the methods, materials and technologies used in the development of the prosthesis.
- **Chapter 5 - Results and Discussion:** details and discusses the findings obtained during the development of the prosthesis.
- **Chapter 6 - Conclusion**: summarizes the key achievements and suggests future work directions.

The research work described in this dissertation was carried out in accordance with the norms established in the ethics code of Universidade Nova de Lisboa. The work described and the material presented in this dissertation, with the exceptions clearly indicated, constitute original work carried out by the author.

2

Theoretical Concepts

This chapter presents the essential theoretical concepts for the development of this project. The first section describes the upper limb anatomy. The second section explores upper limb deficiencies and their different types. The third section discusses AM, the primary technology employed in this work. The fourth section addresses the different types of prostheses, detailing their advantages and disadvantages. Finally, the key challenges in transhumeral prosthetics are emphasized.

2.1 Upper Limb Anatomy

2.1.1 Upper Limb Osteology and Arthrology

The upper limb is a complex part of human anatomy that contains thirty-two bones in total – clavicle, scapula, humerous, ulna, radious, eight carpal bones, five metacarpal bones and fourteen phalangeal bones. It has four groups of joints – shoulder joints (glenohumeral, acromioclavicular and sternoclavicular), elbow joints (ulnohumeral, radiocapitellar and proximal radioulnar), wrist joints (radiocarpal, ulnocarpal, distal radioulnar and scapho-trapeziotrapezoid) and finger joints (carpometacarpal (CMC) joints, metacarpophalangeal (MP) joints and interphalangeal joints), each responsible for a certain movement [4, 5]. The bones and joints of the upper limb are represented in Figure A.1, with the bones shown in blue and the joints in black. Table 2.1 shows standard human ranges of motion of some upper limb joints that are relevant for this work [4, 6, 7].

2.1.2 Upper limb Myology and Movements

There are twenty-six main upper limb movements, performed at shoulder girdle, shoulder, elbow, wrist and fingers levels, which are described in Table A.1, [7, 8]. Shoulder and shoulder girdle movements are coordinated. For example, flexion and extension of the shoulder involve the abduction and adduction of the scapula, respectively [8].

These movements are possible due to the action of the upper limb muscles. Shoulder flexion involves the anterior deltoid, the coracobrachialis, the pectoralis major and, partly,

the biceps. Shoulder extension involves the posterior deltoid, the latissimus, the teres major and, partly, the triceps. Abduction of the scapula, coordinated with shoulder flexion, involve the pectoralis major and minor and the serratus anterior. Adduction of the scapula, coordinated with shoulder extension, involve as principal muscles the latissimus, the trapezius and the rhomboids [8]. Table A.2 contain additional information on the muscles mentioned above, which are the ones that have more interest for this work.

Table 2.1: Ranges of motion of upper limb joints [4, 6, 8].

Joint/Group of joints	Motion	Angles
Shoulder joints	Internal Rotation	0 - 90°
	External Rotation	0 - 20°
	Flexion	0 - 180°
	Extension	0 - 45°
Elbow joints	Flexion	0-145°
	Extension	145 - 0°
	Pronation	0 - 90°
	Supination	0 - 80°
Thumb Carpometacarpal joint	Radial Abduction	Contact - 60°
	Radial Adduction	60° - Contact
	Palmar Abduction	Contact - 45°
	Palmar Adduction	45° - Contact
Metacarpophalangeal joints	Flexion	0 - 90°
	Flexion (Thumb)	0 - 55°
	Hyperextension	0 - 45°
Proximal Interphalangeal joints	Flexion	0 - 100°
	Extension	0°
Distal Interphalangeal joints	Flexion	0 - 80°
	Extension	0°
Thumb Interphalangeal joint	Flexion	0 - 80°
	Hyperextension	0 - 15°

2.1.3 Human Grasp Types

A human hand comprises twenty-three joints, resulting in twenty-seven Degrees of Freedom (DOFs) [4, 9, 10]. This allows the hand to assume several shapes, tailored to various activities or objects being manipulated. Grasp types are commonly used to describe different hand manners of handling an object, and different grasp classifications have been proposed in the literature over the years [9, 11].

Besides the two more consensual categories - power grasp and precision grasp - there is a third category known as the intermediate grasp, which incorporates elements of both power and precision in approximately equal proportions. Power grasps involve using the fingers and palm to hold an object firmly, whereas precision grasps use only the fingertips to stabilize an object [9, 11]. In Table 2.2 there are represented some types of existent hand grasps that are common among prosthetic devices.

Table 2.2: Some types of existent hand grasps [9].

Grasp Classification	Grasp Type		Real Life Application
Power	Cylindrical Grasp (Large Diameter)		Holding a bottle
	Cylindrical Grasp (Small Diameter)		Holding a pen
	Spherical Grasp		Holding a ball
	Disk Grasp		Grabbing a cookie
Intermediate	Lateral Pinch		Using a key
Precision	Tip Pinch		Picking up a coin
	Prismatic Finger		Using a pencil
	Precision Disk		Holding a mug from top
	Inferior Pincer		Holding something between thumb and index finger

2.2 Upper Limb Deficiencies

Limb deficiencies can be either congenital or acquired. Congenital limb deficiencies imply that the person is born with an incomplete limb or with no limb and they are ranked as the second most common birth defect observed in neonates [12]. These deficiencies arise from complications in limb development, a process that occurs between 4 and 8 weeks of gestation [13]. The causes of these complications are difficult to identify, but some of them include genetic disorders, chromosomal mutations, and the exposure to certain medications [14]. On the other hand, acquired limb deficiencies, also known as amputations, result from surgical interventions due to trauma, injury, or disease (mostly tumors, infections, and vascular malformations). Ninety percent of acquired amputations involve only one limb, but they can involve both of them, resulting in a bilateral amputation [15].

When talking of amputations, forearm deficiencies are commonly referred to as transradial amputations or below-elbow amputations. Similarly, upper arm deficiencies are commonly known as transhumeral amputations or above-elbow amputations. Analogously, upper arm total deficiency is known as shoulder disarticulation, forearm total deficiency as elbow disarticulation, carpal total deficiency as wrist disarticulation and phalangeal total deficiency as transcarpal. Different types of upper limb deficiencies and amputations are both represented in Figure A.2 [16–18].

Concerning adults, the predominant cases of upper limb deficiencies are acquired, with trauma and injuries as the most common causes. Moreover, transhumeral and transradial amputations have been revealed as the most prevalent types of upper limb amputations [17, 19, 20]. In contrast, focusing on children, congenital limb deficiencies

are more common than the acquired ones. Among the acquired cases, trauma resulting from traffic accidents and electrical burns are the most common causes. Additionally, among children the most frequent levels of upper limb deficiencies are also transradial and transhumeral, and the incidence of upper limb deficiencies is twice as high as that of lower limb's [21, 22].

2.3 Additive Manufacturing

Additive Manufacturing (AM), also known as 3D printing, is a fabrication technique for producing structures from Three-dimensional (3D) model data, made with Computer-Aided Design (CAD) software. The 3D digital object is exported as a Standard Tessellation Language (STL) file, and then sliced into Two-dimensional (2D) slices by a slicer software, before being read by a 3D printer. This software will generate a G-code, which is a programming language that will give the printing instructions to the printer [23, 24]. After the printing process, a post-processing stage is necessary.

The ISO/ASTM Committee F42 (International Organization for Standardization/American Society for Testing and Materials Group F42) has defined and classified different AM techniques. These include vat polymerization, material extrusion, powder bed fusion, material jetting, binder jetting, direct energy deposition and sheet lamination [24].

Fused Deposition Modeling (FDM) is a material extrusion technique and is the most widely used technique in 3D printing and the most cost-efficient one [23], having a significant relevance in the prosthetics field. In FDM, a thermoplastic filament is heated and deposited layer-by-layer using a nozzle that moves through the print bed, which gradually descends according with the height of the layer previously solidified. FDM can also build multi-material objects by using different nozzles for each material simultaneously [25]. This technique is low-cost because it uses relatively cheap machines (desktop printers ranging from 150$ for the simplest ones to 20000$ for professional ones [26]) and materials ranging from 15$ to 1000$ per kg, with composite materials being the most expensive [27].

The most used thermoplastics in FDM are Acrylonitrile Butadiene Styrene (ABS) and Polylactic Acid (PLA), but Nylon, Acrylonitrile styrene acrylate (ASA), Thermoplastic Polyurethane (TPU), Thermoplastic Elastomers (TPE), Polyethylene Terephthalate Glycol (PETG) and composite materials (such as carbon fiber or fiberglass composites) are also recurrent [25].

Besides its advantages, FDM also present some drawbacks. It tends to have lower resolution due to the incapacity to reproduce small details, resulting in rough surfaces of the object. Moreover, FDM requires support materials for printing overhanging structures and post-processing techniques to enhance the appearance and the quality of the final object, such as polishing or gap filling [23, 25].

2.3.1 Printing materials

The majority of 3D printed prostheses are built by FDM, with PLA and ABS as the main rigid materials. Regarding flexible materials, TPE and TPU (which is a type of TPE) are the most used ones. Filaflex by ©Recreus [28] and Ninjaflex by ©Ninjatek [29] are two widely used examples.

PLA shows higher yield strength (maximum load that a material can support before deforming permanently when being stretched) compared to ABS and it has a low-melting temperature, which means lower temperatures and less stress during printing, making it easy to print with. On the other hand, ABS requires higher temperatures, which complicates the printing process. Nevertheless, ABS has other mechanical properties such as being lighter and being more flexible at the rupture point (higher elongation), indicating a tendency to deform rather than break. In terms of environmental issues, PLA is biodegradable, while ABS is not and may be toxic [26]. PETG is also a very popular material in FDM due to its superior mechanical strength and resistance, especially when compared to PLA, along with its ductility [30]. Filaflex is available in several hardnesses including 82A, 95A, 70A and more recently, 60A. The Filaflex 82A is the original one and it has an elongation of 650%, i.e., the filament can be stretched up to 650% without breaking. Filaflex 60A has an elongation of 950% . Reciflex, which is a recycled TPU filament made by Recreus, is another option. Its hardness ranges between 96A and 98A, and it makes printed parts sustainable, adding value to the devices [28]. Ninjaflex is also available in different hardnesses, 85A and 83A. Ninjaflex 85A has an elongation of 660% [29]. They are all non-toxic, can be in contact with skin and widely used in prosthetics [26].

2.3.2 Printing parameters

There are different printing parameters to consider, which can be set either by the user or by default by the printing software. These are categorized into print parameters, filament parameters, and printer parameters. Print parameters regulate layers, perimeters, speed and infill (internal patterns). Generally, a better quality is achieved with smaller layer heights and lower speeds. Similarly, a stronger print is achieved with higher infill percentage and more perimeters, although this can vary depending on the object. Filament parameters include filament's properties, such as diameter, density, color, and also include the nozzle and bed temperatures of the printer. Printer parameters mainly regulate the movements of the extruder and nozzle characteristics [31] .

The printing orientation is also important to assure a good printing quality. Different components need different printing orientations, according to their design. Another important aspect is support structures. Some objects may need supports, which are structures used in 3D printing that support the overhanging parts of the object during the printing process and provide the necessary stability, preventing its collapse. It is worth adjusting the orientation of the model in order to reduce overhangs and consequently the amount of supports needed [31].

2.4 Upper Limb Prostheses

There are four different types of prostheses – passive, body-powered, externally-powered and hybrid. Each type offers different advantages and limitations, influencing user's choice, which is based on factors such as the purpose of the prosthesis, functionality and anatomical requirements. As a result, the selection process is highly personalized. Table A.3 provides illustrative examples of commercially available prostheses for each type, aiming to offer a comprehensive review of the available solutions.

2.4.1 Passive Prostheses

Passive prostheses, often referred to as cosmetic prostheses, are designed to appear natural, with a high level of anthropomorphism. Passive prosthetic options are light weighted, require less maintenance and have been shown to highly contribute to psychological improvements for the patient, due to their appearance [3, 32]. These prostheses present some disadvantages due to the absence of active components, which means they cannot perform complex movements or be directly controlled by the user. These limitations make them less suitable for a lot of activities when compared to active prostheses (body-powered or externally-powered).

2.4.2 Externally-powered Prostheses

Externally-powered prostheses, also known as electrically-powered prostheses, use motors powered by a battery system to perform movements. There are several control methods, but the most common one is through electromyography (EMG) signals [33]. Prostheses controlled by EMG signals are called myoelectric prostheses. These prostheses are equipped with electrodes that capture electrical signals, generated by the contraction and relaxation of the amputee's residual limb muscles. Then, these captured signals are transmitted to a microcontroller, which triggers the prosthesis movements [32]. Other methods include electroencefalography (EEG) signals or switches [34].

Operating an electrically-powered prosthesis requires the patient's capability to manipulate the device and the ability to understand and control its functions. Moreover, these prostheses have high weight, high initial costs (which can go from 25000$ to 75000$ for upper limb prostheses [35]), increased maintenance requirements, such as battery replacement and repairs, leading to additional expenses. Also, most of them require a controlled environment that is dry, clean and non-corrosive [33, 36]. Despite these challenges, electrically-powered prostheses offer a lot of advantages, such as the enhanced overall functionality, with high grip force and the ability to control different components simultaneously. They also provide comfort and the capacity to control applied force, based on the muscle contraction, in the case of myoelectric prostheses [33].

Transhumeral prothesis are mainly found in the externally-powered prosthetics market. The available options typically involve assembling different modules, including an upper

arm, an elbow joint, a forearm, a wrist joint, and a terminal device (hand or hook). These modules are often compatible with several components from the same distributor or different ones, providing a larger range of solutions [3, 32, 37] .

2.4.3 Body-powered Prostheses

2.4.3.1 Operating principles

Body-powered transhumeral prostheses, which are activated by the body, usually include a harness, a cable, a socket and a terminal device, which can be a hand or a hook. Upper arm, shoulder, back and chest movements are captured by a harness/cable system, allowing the opening and closing of the terminal device (the most common movement in body-powered prostheses) [3, 32, 34]. A scheme of the main elements of a body-powered transhumeral prosthesis is illustrated in Figure 2.1.

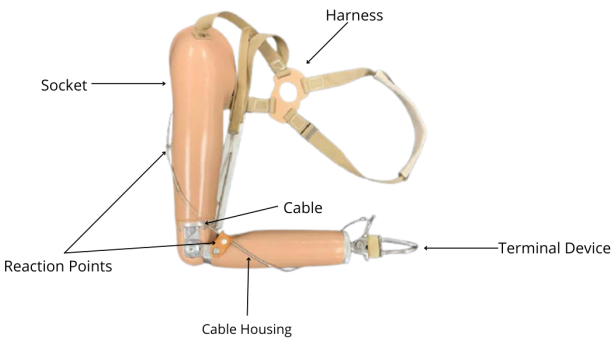

Figure 2.1: Main elements of a transhumeral body-powered prosthesis. Adapted from [38].

The primary body-control motion used is a combination of shoulder flexion and scapula abduction. The residual limb is moved away from the body in the sagittal plane, increasing the distance between the harness and the socket, while the wire is being pulled. Typically, in an average-strength male amputee these motions can achieve a cable excursion of 53±10 mm and an upward force of 280±24 N [39]. In children, these values are significantly lower. For example, in a 5-year-old, the force ranges between 30 and 55 N, based on values recorded in transradial amputees. Additionally, Shaperman et al. state that a seven-year-old child uses 50% to 100% of her maximum available muscle force to operate her prosthesis, in contrast with adults, who use 50% or less [40]. There is no available information about cable excursion in pediatric prosthetics.

The most common cable used in transhumeral prosthesis is a Bowden cable, which consists in a inner tension cable made of twisted steel wire and a outer housing. One example of these cables are bike break cables,where the mechanism is similar: mechanical force is transmitted by the movement of an inner cable within a hollow outer cable

housing. It should be fixed at least in two positions, that work as reaction points for force transmission. Friction is a major cause of force loss in mechanisms like this, so it is important to ensure that the Bowden cable's housing is appropriate and allows the cable to slide easily through it. [41].

2.4.3.2 Voluntary opening and voluntary closing terminal devices

Regarding terminal devices, there are two main types: Voluntary opening (VO) and Voluntary Closing (VC). For VC devices, the default position is the open position, and for VO devices, the default position is the close position.

The VC devices operating method is more similar to natural hand prehension, and the applied force by the user is directly correlated with the output force. However, they require constant tension in the control cable to sustain a constant grasping force, like how the human hand must apply force to maintain a grip. Unlike the human hand, which can easily sustain a grip for extended periods without losing strength, achieving this with devices is more complex. VC devices often incorporate automatic or manual prehension locking mechanisms to address this challenge, which prevents the patient from fatiguing when holding something for a long period of time. On the other hand, a VO device does not face this issue, the object being held only needs to withstand the maximum closing force of the device [39].

2.4.3.3 Whippletree mechanisms

Most hands in body-powered arm prostheses are controlled by a whippletree mechanism. This mechanism is designed to distribute force equally trough a linkage system. The main element of this mechanism is an actuator, where force is applied in one direction at the center and in other directions at the tips. In prosthetics, the force from the actuator is evenly distributed to all the fingers. More complex whippletree mechanisms can be developed by arranging actuators in series, which can provide increased control and flexibility to the system, thus creating a multiple-pulley setup [42, 43]. Furthermore, these mechanisms can vary in dimensional space (2D or 3D), shape, means of force transmission and arrangement of linkage [44].

An example of a whippletree mechanism commonly employed in prosthesis uses bars as actuators and strings as linkage [44]. There are several examples already implemented in hand prostheses, some of which are outlined in Table A.4.

2.4.3.4 Advantages and disadvantages

This type of prostheses is often produced by 3D printing, which provides several advantages. When compared to alternative options they are lighter, more durable, more tolerant to environmental conditions and require less maintenance, with lower costs associated. Despite these advantages, there are some drawbacks, including limited functionality, with insufficient grip force and slow movements. Additionally, they require

more energy to operate, sometimes the mechanism does not work correctly and, generally, they have no anthropomorphic features [33].

2.4.4 Hybrid Prostheses

Hybrid options that combine two prosthetic types in a single device are also available. Body-powered elbows do not necessarily need to be paired with a body-powered terminal device. The most common hybrid device combines a body-powered elbow with an electrically-powered hand [33, 36]. Hybrid prostheses can have better functional outcomes, as they are lighter than a fully externally-powered prosthesis and offer a higher grip force than fully body-powered prostheses [33].

2.5 Main Challenges of Transhumeral Devices

Currently, there is a scarcity of solutions for transhumeral amputations that successfully combine aesthetics, confort, functionality, and low costs. This, along with the previously discussed limitations, contribute to the high rejection rates associated with the use of prostheses. Over the past 25 years, mean rejection rates of 45% and 35% have been observed in studies for upper limb body-powered and externally-powered prostheses, respectively, in children. Regarding adult populations, lower rejection rates were verified (26% and 23% respectively) [45]. The reasons for these rejection rates vary with the type of prosthesis. Some factors include excessive wear temperature, abrasion of clothes, mechanism failure or breakage, unattractive appearance, discomfort, price and durability [46]. Shoulder and neck pain are also very recurrent complaints among amputees wearing prostheses [20].

Additionally, transhumeral prosthesis represent a significant challenge due to the extensive range of motion of the upper limb, which means these prostheses require multiple DOFs, which is difficult to achieve. Their functionality is frequently limited, especially in the body-powered ones, and users often find them challenging to control due to their demanding nature and lack of intuitiveness[47]. Therefore, there is a lack of options for transhumeral prosthesis in the body-powered prosthetics market.

Regarding body-powered VC terminal devices, especially those with five independent moving fingers, they are not widely used. Most commercially available devices in this category are hooks or hands with a moving thumb, as these require less complex mechanisms. Several entities have been developing VC hands with five independent moving fingers, but various challenges have been identified, particularly in improving the grasping force [48].

Given these challenges, it is important to develop a prosthesis that comprehensively addresses all the users' needs. Creating a solution that combines aesthetics, functionality, comfort, and affordability is essential in mitigating rejection rates and ensuring the use of transhumeral prosthetics, which is what this project intends to do.

3

State of the Art

This chapter presents key contributions to the field of prosthetics, that alaign with the main goals of this study. A literature review of existing 3D printed devices that inspired this work is presented and discussed, along with potential improvements that could enhance their functionality. Although there is a notable gap in the development of full transhumeral prosthesis, a wide variety of terminal devices and other modules is available. All the mentioned prostheses are summarized in Table B.1.

3.1 e-NABLE Prostheses

The e-NABLE program is an online worldwide community of volunteers dedicated to developing low-cost, personalized 3D printed prostheses. It currently provides solutions for three types of amputations – transradial, wrist disarticulation and partial hand [2].

E-NABLE designs for transhumeral amputations are currently a work-in-progress. Nevertheless, they offer No-Insurance Optimized Prostheses (NIOP) that are in constantly evolving with the community's input. One of these prostheses is the *NIOP TH-S* [49], which is an upper arm prothesis to help patients who have a working shoulder but a short residual limb, shown in Table B.1. This prosthesis optimally provides eleven DOFs: nine responsible for finger opening and closing, one for elbow flexion and extension, and one for internal and external rotation of the shoulder. The hand movements are controlled by shoulder flexion and scapula abduction, trough a cable that passes through the entire prosthesis, while the remaining movements are manually adjusted, with two locking systems to set the desired elbow position and a third one to hold the hand's grip position [50].

However, this prosthesis faces several challenges when resized, printed, and assembled, as highlighted in C. Patrão's master thesis [50]. In her work, C. Patrão attempted to convert the *NIOP TH-S* into a myoelectric prosthesis, using the same clinical case addressed in this project. Unfortunately, the *NIOP TH-S* did not achieve the desired functionality, particularly regarding hand movements (opening and closing of the fingers) [50]. Another issue concerned the locking systems, which rely on 3D printed parts inserted into the

device to lock it into the desired position. The task of manipulating these components proved to be challenging, particularly for a child. Additionally, the locking system that should hold the hand's grip position, did not work [50]. In conclusion, the hand movements can not be triggered by the user and the remaining ones are difficult to perform. Thus, a reevaluation and improvement of this device is necessary.

As the main issue regards the hand, a potential solution could be replace it with the *Kinetic Hand* [51], which is another body-powered e-NABLE prothesis, fully functional, that has been tested in different clinical cases, represented in Table B.1. To address the elbow flexion mechanism, a possible option could be integrating an alternative e-NABLE elbow, depicted in Table B.1, which demonstrates high functionality in its flexion mechanism. It consists in a pin with an attached spring that when compressed allows for elbow movement and when decompressed locks the elbow in the desired flexed position. This model was presented by the e-NABLE founder, Jonh Schull, in a workshop promoted by the 3D Printing Center For Health in NOVA School of Science and Technology.

3.2 Prostheses with flexible materials

Flexible materials can have different purposes such as simulate soft tissues, skin, enhance aesthetics, increase grasping capabilities and help in bending, contributing to the overall comfort of wearing a prosthesis, without compromising the device's functionality, due to their enhanced mechanical flexibility [52].

Several studies have been conducted in this direction, aiming to integrate flexible materials into prostheses and providing insights for further work. Examples of these studies include master theses by A. Oliveira [53] and F. Pinheiro [54], which focus both on body-powered hands and V. Lopes's master thesis on a passive arm [16]. These works have contributed to the advancement of the field, particularly in the use of PLA for rigid parts and Filaflex for flexible components. A. Oliveira developed a prosthetic hand, in which the fingers were a single piece made by Filaflex, to resemble human fingers, shown in Table B.1. According to her study, Filaflex 70A was the only variant that exhibited some functional capabilities (bending), but she also showed the necessity for some division in the fingers for effective bending, highlighting that flexible material alone might not be sufficient. This gap has already been addressed by the design of the *NIOP TH-S*'s hand ("Kwawu Hand") and the *Kinetic Hand*, both composed by rigid materials in their fingers. Despite potentially compromising the aesthetic appearance and deviating from the realistic shape of natural fingers, these alternatives present a viable solution, benefiting from flexible materials for finger bending. However, with the introduction of the new Filaflex 60A, there is potential for its use in A. Oliveira's finger design due to increased flexibility when compared to the ones that were used. Regarding printing parameters for Filaflex, A. Oliveira explored several combinations to find the best result for the fingers. These combinations can be useful for others working with Filaflex, as it involves a complex

process of trial and error. Ninjaflex, according to F. Pinheiro's and V. Lopes' master theses, is associated with numerous printing issues, which makes it an unsuitable choice [16, 54].

In prostheses with fingers composed by different rigid pieces such as the "Kwawu Hand", findings from C. Patrão's research indicate that, for finger hinges, Filaflex 82A performs better than Filaflex 95A, as it can provide some movement to the fingers [50]. Despite these findings, the fingers still could not bend properly. Therefore, a redesign of the hand is needed to achieve a functional terminal device and continue C. Patrão's work on myoelectric prostheses.

3.3 Prostheses with rigid materials

Regarding 3D printed prostheses made entirely of rigid materials, the *ARM3D*, shown in Table B.1, is a notable example. Developed by Madelon M.A. Kusters in his master thesis [55], this prosthesis aimed to address the gap of transhumeral prostheses in the body-powered market. The *ARM3D* has three DOFs, a VC hand, a wrist rotation mechanism and an elbow flexion mechanism. The wrist rotation mechanism is based on the same principle as the previously mentioned e-NABLE elbow and demonstrates high functionality. Another advantage of the *ARM3D* is its superior finish, achieved through the use of Polyvinyl Alcohol (PVA), a water-soluble material, as a support material alongside PLA, which eliminates the need for post-printing processing [56]. The control cable is a bike brake cable and runs internally through the prosthesis, which is a good feature to adopt in future works. However, the device has some limitations: it has only four moving fingers, while the thumb is fixed in one position, and the fingers move together as a single unit without independent movement. These issues should be addressed to enhance its grasping capabilities. Furthermore, the hand design could be refined to achieve a more anthropomorphic appearance and flexible materials could be introduced, specially in the upper arm part, to improve comfort.

Another notable prosthesis is the *Touch Hand II Prosthetic Hand*, developed by G.K. Jones et al. [57] and shown in Table B.1. This prosthetic hand can be combined with a wrist and socket to create a transradial device. It is electrically-powered by motors but is manufactured by AM. This prosthesis offers fourteen DOFs, which is a very good result. It uses a pulley system across the fingers, what significantly improves force transmission. However, the design lacks an anthropomorphic form, and the fingertips would benefit from a rubberized surface to improve grasping and prevent objects from slipping. The primary material used is ABS, which is not biodegradable, and the inclusion of various metals adds weight to the device. The mass of the hand, including electronics and the wrist but excluding the socket, is 486 g.

Both of these prostheses were developed through comprehensive studies that included a wide range of tests, such as grasp type tests, tensile tests, closing tests, pinch tests, grasping force tests and FEA. The methodologies and findings of these studies have directly inspired the product validation phase of this work.

4

Methodology

The methodology used in this work was inspired in the *Product Design and Development* methodology [58]. The first step was the concept development, with the identification of the main challenges in upper limb prosthetic devices, described in Chapters 2 and 3. This also included the identification of the case-study child's needs along with other children with similar conditions. Then, the product development began with the remodeling of the *NIOP TH-S* to meet the acquired specifications. Several prototypes were designed in *Fusion 360* and *Solidworks* software, printed and tested, ensuring an iterative improvement of the prosthetic device. Finally, for product validation, the final prototype was evaluated in terms of resistance and performance, with several tests and Finite Element Analysis (FEA). Measurements of the case-study child were taken and a 3D scan was performed to establish the dimensions of the final product. To conclude, the final prosthesis went under evaluation with the case-study child, to access its functionality, strengths and weaknesses.

4.1 Concept development

In addition to identifying the primary gaps in upper limb prosthetics through external research, present in Chapters 2 and 3, detailed insights were also gathered directly from patients and professionals at Hospital Dona Estefânia, enriching the understanding of specific needs and complaints. These insights are detailed below.

According to the highly experienced team in treating children with congenital malformations at Hospital Dona Estefânia, one of the primary needs for amputees is comfort, which can be easily achieved through the use of flexible materials. Unlike rigid materials, which may require foam or other protective measures to mitigate discomfort or skin irritation, making the device less practical to correctly apply and increasing body temperature, flexible materials provide a more comfortable fit. Anthropomorphism was also highlighted as crucial in helping amputees feel integrated into society, as it influences how they perceive themselves and interact socially. It is also important to build the prosthesis with appropriate height, to prevent future posture and asymmetric problems. Another significant concern, especially for children, is the need for frequent prosthesis changes due

to growth. In this regard, 3D printing offers a promising solution as it allows quick and easy adjustments to accommodate growth. Another issue arises when children can easily remove their prostheses, increasing the likelihood of using them as toys rather than for their intended purpose. Therefore, it is crucial to incorporate a secure mechanism to hold the device in place. Moreover, upper limb prostheses should be designed to meet a diverse range of needs, aiming to minimize the requirement for multiple devices. Alternatively, prosthetic designs could incorporate features such interchangeable terminal devices, for instance, replacing a hand with a support device to a specific activity. Another important feature highlighted was the ability to rotate the terminal device, what can be helpful in different activities for children. After identifying all these challenges, the specific needs of the case-study child were also determined. She requested a skin-colored prosthesis with a comfortable, non-itchy socket, a lightweight design, and the ability to perform hand closure. Finally, the primary concepts for the development of the prosthesis were generated based on the collected information.

4.2 Product development

4.2.1 Existing Issues

The *NIOP TH-S* prosthesis was selected as the starting model. Its components are divided into four sections - "Kwawu Hand", "Standard Wrist Pin", "Shelbow" and "XO-Shoulder" - and are illustrated in Figure C.1. The STL files of these components were downloaded from e-NABLE's website [49] and redimensioned using *OpenScad* software, according to the case-study child's measurements and to the parameters outlined in Table C.1. Subsequently, the resized files were printed and assembled following the assembly guide also provided on e-NABLE's website [49]. During this process, the issues previously identified by C. Patrão [50] were studied, leading to the elimination of some features, while considering other alternatives.

The redimensioning process encountered several issues, with certain components failing to be accurately resized. This required design modifications in the wrist components, "Palm", "Forearm", "Dowels", "Shelbow Lateral", "Shelbow Medial", "Humeral Bottom Plate", and "Hinges", implemented both in *Fusion 360* and *SolidWorks* software.

Furthermore, the assembly revealed numerous challenges, particularly at the hand level. The holes intended for the wire were too small and had complex configurations, blocking the passage of the wire. Polyester wire proved almost impossible to thread through the holes, requiring the use of a stiffer nylon wire, sometimes even guided by a metallic wire. Additionally, several parts of the prosthesis required polishing to ensure proper fit, and almost all holes needed enlarging for screws. Moreover, certain parts did not fit together perfectly, compromising stability.

After the assembly, functionality issues emerged. Concerning the hand, the fingers only presented some reduced and very limited movement, being unable to close. In

conclusion, at the hand level, besides the holes, the whippletree mechanism, represented in Figure 4.1, also needed to be modified. This mechanism could be one of the factors contributing to the limited movement of the fingers, as either the distribution of force from the actuator to the fingers might not be optimized or the force gained in the actuator might not be sufficient to move the fingers.

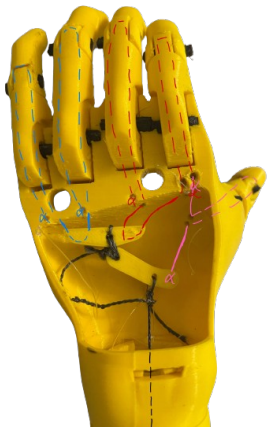

Figure 4.1: Whippletree mechanism of the "Kwawu Hand". Blue line represents the wire through the pinky and ring fingers. Red line represents the wire through the index and middle fingers. Pink line represents the wire through the thumb. Black line represents the main wire.

In the "Shelbow" region, instability was observed, which could potentially be addressed by replacing the "Dowels" for a through bolt. Moreover, the elbow flexion locking mechanism did not show good functionality, requiring the screw to be slightly loosened for the "Pin with switch" to move into the unlock position, yet this compromised stability. Furthermore, the shoulder rotation locking mechanism, despite being a good mechanism, demanded excessive force, beyond what an eight-year-old could exert. Regarding all of that, the "Shelbow" region should also be redesigned and improved, along with the hand. The grip locking system, situated in the forearm, failed to operate. Its intended purpose was to hold the hand's grip position by compressing the string, yet it did not achieve this function. Regarding the forearm shape, it was too thin and cylindrical and could be improved. The "XO-shoulder" region benefits from thermoforming to mold the "Arm wrap" and "Shoulder Connector," what ensures a perfect fit of the device on the child's stump. However, it exhibited poor structural integrity and required tightening, as the "Arm Wrap" easily slipped.

For the first prototype, represented in Figure 4.2, PLA was used in all the components (except in the finger "Hinges", which were made by Reciflex). Nylon wire (diameter 0.26 mm, resistance 7 kg) was used in the fingers, and polyester wire (diameter 0.60 mm, resistance 62 kg) was used to connect the hand to the remaining components of the prosthesis. The sole purpose of this first prototype was to get a better understanding of the device's existing problems found by Patrão [50] and determine possible solutions. Therefore,

default printing parameters were used and filament colors were chosen according to the laboratory's availability.

(a) Anterior View (b) Posterior View

Figure 4.2: First prototype.

4.2.2 Design

Design alterations made to the first prototype went from distal to proximal order contradicting the norm. This approach was taken because changes in the proximal region could have repercussions in the distal area.

4.2.2.1 Hand

First, several whippletree mechanisms, inspired by those in Table A.4, were designed, printed, and incorporated into the *NIOP TH-S*'s hand to assess potential improvements in functionality.

In a second phase, the *Kinetic Hand* design was taken into consideration. The following modifications were made to the original design: incorporation of the whippletree mechanism inside the hand structure instead of being outside, a redesign of the wire arrangement, and a connection between the palm and the wrist. The modified palm can be seen in Figure 4.3a. The palm cover was completely redesigned to get a more anthropomorphic form, with hand palm shape, and it is shown in figure 4.3b.

(a) Original and modified palm. (b) Original and modified palm cover.

Figure 4.3: Design modifications made to the *Kinetic Hand*.

4.2.2.2 Forearm

A 3D scan of a forearm was conducted with the *EinScan H2 Handheld 3D Scanner* from ©Shinning 3D to capture precise anatomical surfaces and geometry, aiming for a more anthropomorphic result. Given the impracticality of scanning the child's forearm, an adult one was used instead. The scanned file was initially processed on *Shining 3D* software, then resized and treated like any other STL file. The scan, on the left, and its CAD design, on the right, are shown in Figure 4.4. Also, the movements of pronation and supination of the elbow were added to the forearm, with the creation of a 360° rotation mechanism, also visible in Figure 4.4.

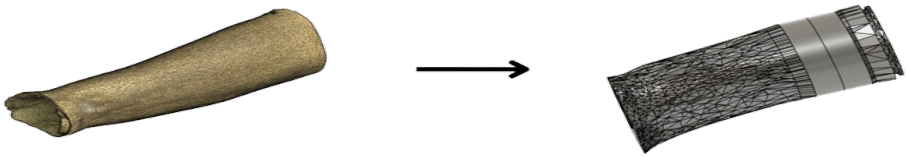

Figure 4.4: Design modifications made to the forearm scan.

4.2.2.3 Elbow

Regarding the elbow, the goal was to incorporate a functional flexion mechanism into the *NIOP TH-S*'s design. The mechanism was inspired by the e-NABLE elbow presented in Section 3.1 , displayed in blue in Figure 4.5. Design changes were made on every component of the "Shelbow" region and two new parts were introduced, the "Puller" and the "Cap", with their drawings presented in Appendix E. Additionally, the "Dowels" were replaced with a through bolt to provide more stability to the entire region. The CAD designs of the new elbow and its flexion mechanism are shown in figure 4.5.

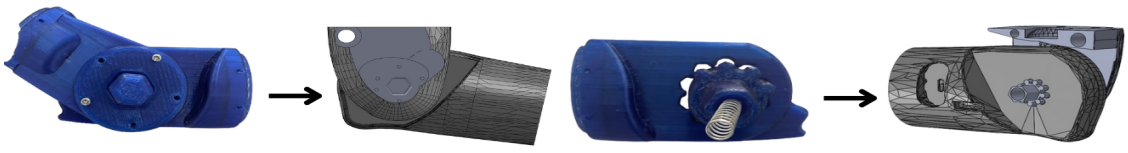

Figure 4.5: CAD design of the new elbow based on the e-NABLE elbow.

4.2.2.4 Shoulder

The shoulder region suffered alterations in the "Arm Wrap", "Scapula plate" and "Humeral Latch Pin". The "Arm Wrap" was extended and a structure to hold cable ties was added, as shown in Figure 4.6. In the "Scapula Plate", the corridor where the wire

passes was repositioned. The shoulder rotation mechanism was retained, requiring only a size reduction of the "Humeral Latch Pin".

In prototyping, the "Arm wrap" was thermoformed using a hair dryer as heat source, without molds. For the final product, a heat gun was used instead along with a 3D printed mold with the dimensions of the case-study child limb, shown in Figure C.2. The "Shoulder Connector" was thermoformed directly on the child's shoulder during the fitting of the prosthesis.

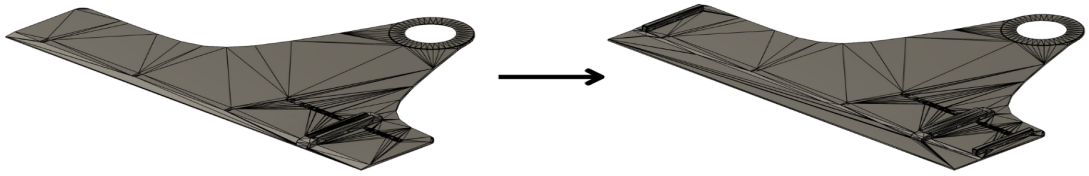

Figure 4.6: Design modifications made to the "Arm Wrap".

4.2.3 Measuring and scaling

The measurement collection of the case-study child's upper limbs was conducted in collaboration with the child's grandfather. The detailed procedure is shown in Figure C.3, with the results in Table C.3. In the prototyping phase, the measurements previously taken by Catarina Patrão [50] (shown in Table C.2) were used. For the final product, these were updated to the most recent ones, collected during this study. The new collection included a more extensive list of measurements compared to the oldest one.

This prosthesis was designed for a left-arm amputee, but it can also be printed for right-arm amputees using the mirror function in *PrusaSlicer*. This software also includes a scaling function, allowing for easy size adjustments. This method was employed to scale the final prototype, made according to last year's case-study child measurements, to fit the new measurements. In general, a uniform scaling of 123% was applied to the components across x, y, and z axes. However, for components that required more precise adjustments, non-uniform scaling was applied using *SolidWorks* and *Fusion 360* software.

4.2.4 Printing

4.2.4.1 Materials

In the prototyping phase, all components were printed with PLA, except the "Hinges", "Grips" and "Palm Cover", which were printed with Reciflex. The filament colors were according to the laboratory's availability. For the final product, 98A TPU was used instead of Reciflex, and both filaments, PLA and 98A TPU, were chosen in a nude color to simulate the human skin.

A third filament, Filaflex 82A, was also tested on the finger "Hinges", "Grips" and "Palm Cover". Additionally, the introduction of flexible materials in other components was also

tried. Some of them showed good results but were not included in the final product for the case-study child, while others performed poorly. These results are all detailed in Chapter 5.

4.2.4.2 Printing parameters

The 3D printers used for this project were the Original Prusa i3 MK3S+ and the Original Prusa Mini by ©Prusa. Printing parameters were defined using the *PrusaSlicer* software.

PLA components were initially printed using the default "Generic PLA" settings for filament and the default "0.20mm SPEED" settings for print. For the final product, the "0.15mm QUALITY" settings were used to enhance detail. TPU components were printed using the default "Generic Flex" settings for filament (with the bed temperature reduced to 0 ºC) and the "0.20mm SPEED" settings for print, initially. For the final prototype, the "0.15mm QUALITY" settings were used. Filaflex 82A components were printed with parameters based on those found by Ana Oliveira[53]. All the used parameters are listed in Table C.4.

The infill percentage, which determines the density of the object's infill, was set at 15% for most components, while the "Puller," "Cap," "Pin," "Grip lock switch," "Humeral core," and "Humeral top plate" parts were set at 40% due to their need for increased strength.

4.2.5 Assembly

The different components that compose this new prosthesis are illustrated in Figure 4.7, divided into four sections - "Shoulder", "Elbow", "Forearm", "Hand". The assembly of this prosthesis was based on the *Kinetic Hand* Assembly Manual [51] for the hand and on the *NIOP TH-S* Assembly Manual [49] for the remaining parts, with some alterations given to the new designs and components. The new assembly guide is in Appendix F and contains all the instructions to assembly this new device.

4.3 Product validation

For the product validation phase, an adult-size terminal device was printed. This was obtained by scaling the terminal device with the case-study child dimensions, by 130%, using the *PrusaSlicer* software. Having a small and a larger hand enabled the comparison between prostheses with different sizes.

4.3.1 Mechanical Tests

Mechanical tests were carried out using a universal testing machine from ©Steplab. The testing procedures were based on those conducted by Gerwin S. and Dick P. at The Delft Institute of Prosthetics and Orthotics [59], as well as on the methodologies used by Renato M. et al. [60, 61]. The tests that were performed include:

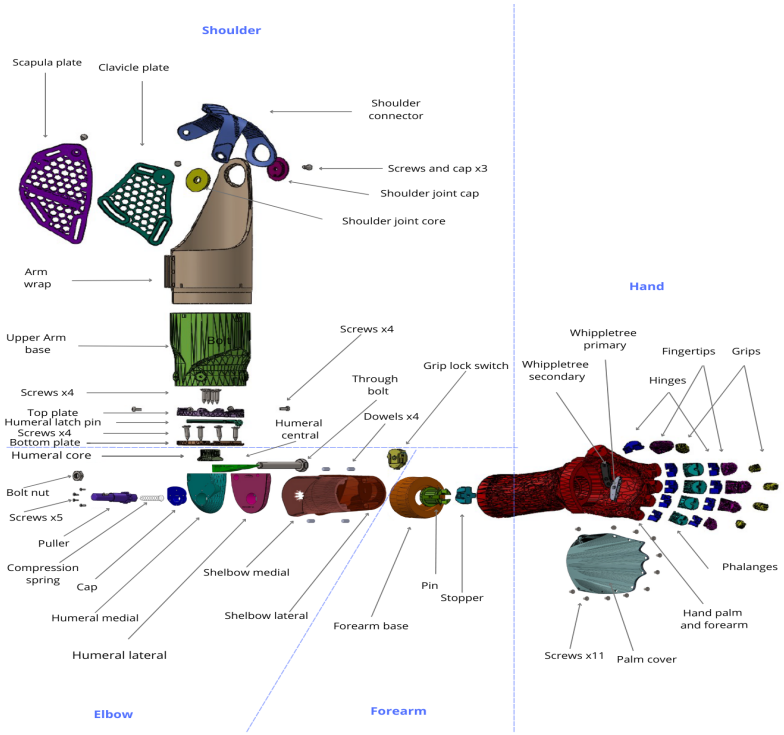

Figure 4.7: Exploded view of the developed prosthesis made with *Solidworks* software.

- **Closing Test** (measuring the activation cable force required to close the hand and measuring the activation cable displacement)
- **Grasping Test** (measuring the activation cable force required to grasp a 10 mm diameter cylinder and measuring the activation cable displacement)
- **Pull Test** (measuring the pulling force for which a 10 mm diameter cylinder is released)

Besides these tests, the work needed to close the terminal device and the work needed to close the terminal device and grasp a 10 mm diameter cylinder were also calculated. The amount of work can be graphically displayed as the area under the force-displacement curve and numerically expressed as:

$$W = \int_0^l F(x) \cdot dx \tag{4.1}$$

in which: W = work (Nm); l = maximum cable excursion (m); $F(x)$ = activation cable force (N); and x = cable excursion (m).

All tests were performed tree times for each terminal device, the small and the larger hand, and average values were obtained for each test. The sampling rate used in the tests was 2 Hz for the small hand, which was the first to be evaluated, and 5 Hz for the larger

hand, as it was verified that there were too many unnecessary points. The motor velocity was 0.5 mm/s for all tests.

The acquired data was processed using *Microsoft Excel* and *MATLAB*. Plots were created to illustrate the relationship between cable displacement and cable activation force, and for the pull tests, the relationship between hand displacement and pulling force. Moving averages were applied to the scattered data of each trial, represented by a line in the respective trial colour, with different periods tailored to each. For closing and grasping tests, a 10-period moving average was applied to all trials. For pull tests, a 10-period average was used for small hand trials, and a 5-period average for larger hand trials, as these had less points and great variations. This method smooths data over time, helping to identify trends in noisy data. The work required for closing and the work required for grasping were calculated in Nmm using *MATLAB* functions. These functions computed the area under each moving average curve, represented in the plots in Section 5.2 as shaded areas in the respective trial colour. An average value in Nm was then estimated for each test.

Since the terminal device is the only part of the prosthesis being evaluated in these tests, the remaining components were removed to optimize the use of the machine and its limited space. The hand position and the wire pulling direction for each test were chosen based on available space and can be visualized in Figures C.5 and C.6. Although these positions differ slightly from those used during actual device operation, the differences are minimal and can be disregarded since the tension transmitted from the wire does not vary significantly with changes in direction. Even if the wire is pulled from a different angle than in real use, the force transmitted to the hand remains practically the same.

To ensure proper test performance, support fixtures were required to securely hold the prosthesis, the cable and the cylinder in place. These fixtures were designed, 3D printed and are shown in Figure C.4.

4.3.2 Grasp Type Tests

To evaluate the various types of grasps that the prosthesis can simulate, multiple trials were conducted involving the grasp types displayed in Table 2.2, using 3D printed and non-3D printed objects of different sizes. The items used in these trials included common objects used in daily living activities - bottles, pencils, pens, mugs, balls, and 3D-printed cylinders and disks. Disk diameters ranged from 40 to 80 mm in 10 mm increments, and disk thicknesses varied from 5 to 20 mm in 5 mm increments. Cylinders (bottles, pencils, pens and 3D-printed cylinders) were tested in small sizes (5 to 20 mm in diameter, in 5 mm increments) and large sizes (40 to 60 mm in diameter, in 10 mm increments) with varying heights that were not a primary focus of these tests. To test whether grasping skills improve with larger dimensions, the larger hand was also evaluated. The results of these experiments are presented in Chapter 5.

Additionally, both hand spans, which consist in the distance from the little fingertip

to the thumb fingertip, were measured with a ruler. This measurement approximately represents the maximum opening width of a hand, which directly influences the grasping capabilities. Hand opening width between the thumb and the index fingertips were also measured in both hands. Both measurements are visually represented in Figure C.7.

4.3.3 Goniometry

Goniometry, the science of measuring joint angles in human articulations [62], was employed to assess the ranges of motion allowed by the prosthesis. These angles were measured using a goniometer, as illustrated in Figure 4.8. The measurements were conducted according to the *Manual De Goniometria Medição Dos Ângulos Artiulares* instructions [62]. Five measurements were taken for each position of the articulation under study, and a mean value was calculated, along with its Standard Deviation (SD).

The device offers eight distinct angle positions for shoulder rotation and three for elbow flexion, all of which were measured. Regarding the hand joints, maximum angles of flexion and hyperextension were studied in both MP and interphalangeal joints. The four distal interphalangeal joints and thumb interphalangeal joint are fixed at an angle, that was also assessed. Additionally, the thumb CMC joint is fixed for both palmar and radial abduction, and these angles were measured as well. Measurements were taken with the hand in maximum closing position by pulling the main wire to study finger flexion and with the fingers fully extended to evaluate finger hyperextension and thumb abductions. All measurements are presented in Chapter 5.

(a) Goniometer in position for elbow flexion measuring.

(b) Goniometer in position for MP joints flexion measuring.

Figure 4.8: Measuring ranges of motion with a goniometer.

4.3.4 Finite Element Analysis

This work uses the Finit Element Method (FEM) to perform a structural analysis on the most critical parts of the device, the fingers, to check for possible load failures. Additionally, FEM was used to study different types of materials for the finger hinges, more specifically, TPU 98A, Filaflex 82A and Filaflex 95A. FEA decomposes a complex structure into a mesh of smaller parts, finite elements, analyzes each one individually, and then combines the

results. It generally involves five steps: material definition, fixtures, forces, mesh creation, running the study and analyse relevant results [57]. *Solidworks SimulationXpress* was used to perform this analysis by assuming a linear static scenario and the results are depicted in Chapter 5.

Material properties of PLA, TPU 98A, Filaflex 82A and Filaflex 95A were not defined in the *Soliworks* library, so they were taken from outsourses and are present in table C.5 [63–67]. The yield strengths of Filaflex 82A and Filaflex 95A were not found in the biliography, so they were roughly assumed to be the same as their ultimate tensile strengths.

The loads were assumed to be static and some faces were fixed according to the configuration of the device. In the simulations, the applied loads are represented by pink arrows and fixed points are represented by green arrows. A load of 10N (1kg) was considered at first as the maximum load that the prosthesis can withstand, according to the pulling force test previously performed in the small hand. Thus, for each finger, the maximum load was assumed to be 2N. However, higher force values were experimented and the index finger handled until 5N, so this value was considered instead. The used mesh consisted in 1.3 mm tetrahedral shaped elements.

The relevant results included information on the Von Mises stress experienced by the components (equivalent tension reduced to a single point), the strain they underwent (deformation per unit length), the displacement observed (how much the material deformed), and the Factor of Safety(FOS). The FOS is a numerical measure to quantify the margin of safety provided by a structure or component. It is defined as the ratio between the maximum stress a structure can withstand under normal conditions and the maximum load it will actually experience during operation [68]. FOS values larger than 1 indicate that the material is safe, under than 1 indicate that the material will fail. FOS calculation is based on a failure criterion. In this study, the used criterion was the Maximum Von-Mises Stress, commonly used in ductile materials analysis[69], such as TPU and Filaflex.

4.4 Product Evaluation

The prosthesis evaluation was conducted with the final product, after the prototyping and testing phases, with the case-study child and her family. The device was properly adjusted and fitted to the child, and it was assessed in terms of functionality and appearance. Additionally, its weight, cost and construction time were estimated using *PrusaSlicer* software. The weight was then validated by effectively weighing it on a scale. All the results are described in Chapter 5.

5

Results and discussion

This chapter presents and discusses the results obtained throughout the entire work. It begins by presenting the results of the product development phase, which involved the creation of several prototypes, stemming from design modifications. It then covers the results related to 3D printing technology and the assembly. Finally, it shows the results of the product validation phase, from the several tests and analyses conducted on the final prototype. After testing the final prototype, the final product was created for the case-study child. The chapter concludes with an evaluation of this product, along with suggestions for further improvements. All the figures correspond to the final prosthesis.

5.1 Product development

5.1.1 Design

This section presents the results obtained from the design alterations made in the "Hand", "Forearm", "Elbow" and "Shoulder" regions of the prosthesis.

5.1.1.1 Hand

The *NIOP TH-S*'s hand needed improvements on the whippletree mechanism. Despite trying several whippletree designs into the "Kwawu Hand", no significant enhancements were observed. Nevertheless, it was deduced that the main issue was the limited space within the hand. The 3D mechanisms allowed a wider range of movement, and the closing was slightly better compared to the 2D counterparts, but still very limited. So, it can be concluded that the "Kwawu hand" does not function optimally for pediatric dimensions. An increased hand size may correlates with improved functionality.

Then, the *Kinetic Hand* was taken into consideration. A huge improvement was seen, as the fingers were able to fully close. This was achieved by using the original "Kwawu Hand"'s whippletree mechanism with a different configuration, positioning the "Whippletree primary" part differently to maximize space and by simplifying the wire arrangement. This new wire arrangement consisted in shortening the original wire path of the *Kinetic Hand*. Instead of looping up and down the same finger, the wire now

passes through it only once, which is sufficient to bend the fingers and avoids conflicts between wires at the common entry hole. This single-loop design was possible by adding a small bar in the fingertip cavities, visible in Figure 5.1c. The new prosthetic hand and its whippletree mechanism are shown in Figure 5.1.

(a) Anterior View (b) Posterior View (c) Whippletree mechanism.

Figure 5.1: Prosthetic hand. (c) Whippletree mechanism. Red line represents the wire through the pinky and the ring fingers. Blue line represents the wire through the index and the middle fingers. Pink line represents the wire through the thumb. Black line represents the main wire.

5.1.1.2 Forearm

The *NIOP TH-S*'s forearm needed to improve its too cylindrical shape, what was done by using 3D scanning technology. Regarding the new elbow rotation mechanism, shown in Figure 5.2, it allows a 360° rotation of the forearm and hand. This feature has been identified as highly significant in pediatric prosthetics, as it can facilitate certain activities. However, it represents an unnatural movement of the elbow joint and to better replicate human forearm functionality, pronation beyond 90° and supination beyond 80° could be restricted.

(a) Mechanism in position. (b) Mechanism's components: Pin and stopper.

Figure 5.2: Rotation mechanism of the forearm.

5.1.1.3 Elbow

The original elbow flexion mechanism needed improvements in order to become more stable and easier to manipulate. The new mechanism allows the elbow to flex at three

different degrees (29.0° , 71.6° , 107.8°) due to the configuration of the device. It consists in a pin designated "Puller" with a compression spring attached at the end, that when compressed, allows movement, and when decompressed locks the current position. Figure 5.3 shows an internal and an external view of this mechanism.

(a) Elbow's exterior. (b) Elbow's interior.

Figure 5.3: Elbow flexion mechanism.

The grip locking mechanism, despite some design changes, still does not work properly. In prototyping phase, it was able to keep the prosthesis closed while not being used, what could be helpful so the fingers do not touch random things, yet it was not strong enough to fully hold a grip position when grabbing something, which should be its main function. However, in the final product, with its larger dimensions, it did not work at all. As a result, it should be completely restructured.

5.1.1.4 Shoulder

The original shoulder region required modifications to enhance security. These design changes significantly improved the device, ensuring that the "Arm Wrap" stays securely in place and no longer slips. Additionally, the performance of the cable mechanism was enhanced. By redirecting the corridor through which the wire passes in the "Scapula Plate", more space was created, allowing the cable to reach a higher excursion.

Regarding the thermoforming process of the "Arm Wrap", the mold that was used was 3D printed in PETG to resist the higher temperatures involved in the process and ensure a more perfect result.

5.1.2 Printing

Printing parameters vary according to the materials used. In this work, printings involved PLA, TPU 98A and Filaflex 82A.

5.1.2.1 Materials

Finger "Hinges" were printed in TPU 98A and Filaflex 82A to compare hand performance. For the final product, TPU 98A was used as it exhibited the best results, providing greater grasping force, which is consistent with the FEA findings detailed in Section 5.2.4.

The finger "Grips" and the "Palm Cover" were also printed in both materials. In these areas, the use of Filaflex can be helpful in manipulating objects due to its greater flexibility compared to TPU 98A. However, the Filaflex filament pigment was not the same as the PLA filament's. So, for the final product, TPU 98A was used instead because it matched the PLA filament color. Aesthetics was prioritized since the difference in the device's functionality between the two options was not that significant.

The "Arm Wrap" and the "Upper arm base" parts were also printed in TPU 98A, besides PLA, to make them as comfortable as possible since these components are in contact with the child's stump. However, functionality was lost, so the PLA versions were retained.

The "Shoulder Connector", the "Scapula plate" and the "Clavicle plate" were also printed in TPU 98A, besides PLA. Although these components were not used in the final product designed for the case-study child, because these were not pointed out as pressure points by her, they were incorporated into the final prototype afterwards. The functionality of the prosthesis was not affected, and the flexible material provided enhanced comfort.

5.1.2.2 Printing Parameters

During prototype development, rougher parameters were used, but the final product prioritized detail. The main differences between the two print settings for PLA and TPU printings ("0.20mm SPEED" and "0.15mm QUALITY") are the layer height and speeds for perimeters and infill. Thinner layer heights and lower speeds result in higher printing quality.

For the Filafex 82A printings, different sets of parameters found by A. Oliveira [53] were tried, specifically sets b6, b5, b, and a2. The best results were obtained with set b6, with an increased infill percentage of 15% (instead of the stated 5%), and the bed temperature reduced to 0 °C. All the parameters that were used are listed in Table C.4

5.1.3 Assembly

Figure 5.4 presents the assembly of the final product that was developed during this study, prior to being fitted to the case-study child.

(a) Anterior view. (b) Posterior view.

Figure 5.4: Assembly of the final prosthesis.

5.2 Product Validation

5.2.1 Mechanical Tests

To validate the final prototype, different tests were conducted on both the small and the larger hands: closing test, grasping test and pull test.

5.2.1.1 Closing Test

Hand closing is a key focus of this work, as it represents one of the primary movements of a prosthetic arm. From the plots shown in Figure 5.5, the values of maximum cable excursion and activation cable force necessary to close the terminal device can be determined.

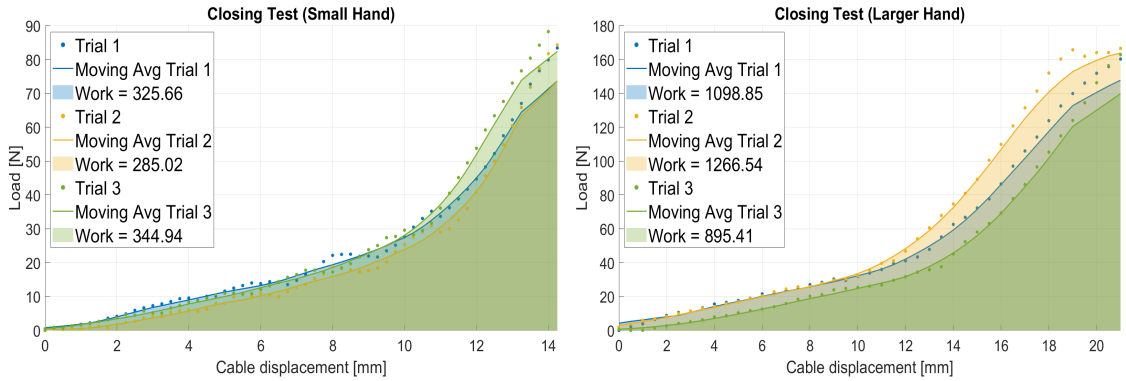

(a) Closing test of the small hand.

(b) Closing test of the larger hand.

Figure 5.5: Closing tests.

Regarding the small hand, the device is fully closed with a cable displacement of 14.3 mm and requires an average activation cable force of 85.3 N. Since a 5-year-old child can exert an upward force of 30-50 N, it is believed that a 8-year-old amputee can achieve this value. Also, since an adult shoulder can achieve a cable displacement of (53 ± 10) mm, it is believed that a 8-year-old can reach 14.3 mm or more.

For the adult-sized hand, the device fully closes with a cable displacement of 21.0 mm and requires an activation cable force of 163.2 N. Given that an average adult can exert an upward force of (280±24) N and reach a cable displacement of (53 ± 10) mm, it is believed that the prosthesis will function effectively in most cases.

In the small hand closing test displayed in Figure 5.5a, variations between 4-12 mm of cable displacement can be observed in the scatterd data. These variations are due to the adjustment of the hand's whippletree mechanism. As the wire is being pulled and the fingers close, the whippletree continuously adjusts itself to redistribute the new load among the fingers. Conversely, in the larger hand trials, these variations are not visible because the loads involved are much higher. Although the whippletree still adjusts itself, the resultant load variations of the process are too small in comparison to the loads involved in the hand closing to be noticeable in the plot.

The average work needed to close the small hand is 0.3 Nm, and for the large hand, it is 1.1 Nm. Therefore, the small hand needs less work (energy form the amputee) to operate than the larger hand, as it was expected.

These tests were terminated when the hand was visually observed to be fully closed in the first trial, which then determined the end conditions for the subsequent trials. It is important to highlight that the tests end conditions were determined visually, so it is normal to have limitations in reaction and action times, although the tests were conducted with the assistance of two participants. This is applied to all the performed tests.

5.2.1.2 Grasping Test

The minimal force necessary to close the fingers and to start building up a grasp force differs among devices. These tests were terminated when it was visually observed that the fingers started firmly pressing the cylinder in the first trial, which then determined the end conditions for the subsequent trials.

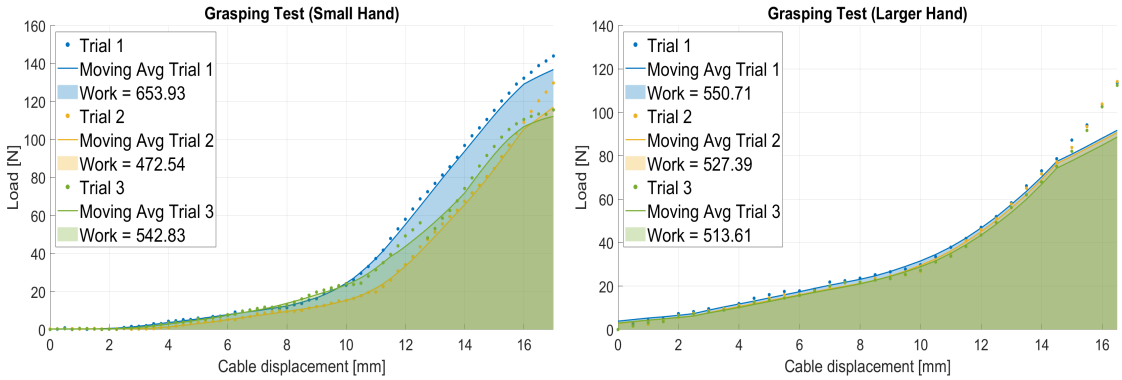

(a) Grasping test of the small hand. (b) Grasping test of the larger hand.

Figure 5.6: Grasping tests.

From the plot shown in Figure 5.6a, the average activation cable force needed to close the small hand and grasp a 10 mm diameter cylinder is 129.8 N. Regarding the larger hand, the average activation cable force needed to close and grasp a 10 mm cylinder is 113.4 N. This happens for approximately 16.5 mm of cable displacement, as displayed in the plot in Figure 5.6b.

In the small hand grasping test, the initial region of the plot is approximately constant, because it encompasses the period before the wire is under tension, what can be attributed to the configuration adopted to pull the wire during this test. The wire becomes fully tensioned near 3 mm, therefore, the actual cable displacement required to close and grasp the object is about 14.0 mm, instead of the 17.0 mm displayed in the plot.

The average work needed to close and grasp a 10 mm cylinder is 0.6 Nm for the small hand and 0.5 Nm for the larger hand. To conclude, for the larger hand, the closing task requires more work than closing and grasping because the fingers do not fully close in the second case, which requires less energy from the amputee (smaller cable displacement

and activation cable force). These findings are in accordance with the results of the study conducted by Gerwin S. and Dick P. on several commercially available VC prosthetic hands [59]. On the other hand, the small hand does not exhibit the same results. The amount of work needed to close and grasp the object is greater than the amount of work needed to only close the device. In this specific case (10 mm diameter cylinder), even though fully closing the device requires a greater cable displacement, the extra force needed to start firmly grasping the object is higher than the force required to just close the device, what leads to a greater work. If the cylinder had a smaller diameter, such as 5 mm, the small hand would likely perform similarly to the larger hand with the 10 mm cylinder, as less force would be needed to firmly grasp it.

5.2.1.3 Pull Test

Pulling force is the force in which an object moves towards the source of the interaction [60]. In these tests, the object (10 mm diameter cylinder) was fixed while the hand was being pulled, as represented in Figures C.5c and C.6c. Given the definition of pulling force, these test results can be approximated to the maximum load that the prosthesis can withstand without failure, which would be measured in a tensile test [60, 61]. Therefore, from the plots shown in Figure 5.7, the maximum loads that the small and larger hand can withstand can be determined.

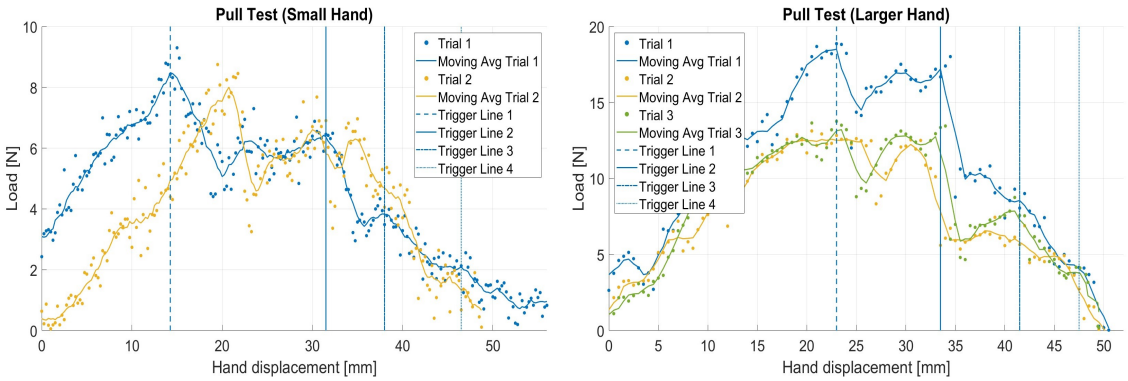

(a) Closing test of the small hand.

(b) Closing test of the larger hand.

Figure 5.7: Pulling tests. Trigger Line 1 represents little finger failure; Trigger Line 2 represents index finger failure; Trigger Line 3 represents ring finger failure; Trigger Line 4 represents middle finger failure.

The irregularities observed in the plots correspond to the failure of individual fingers. Four significant load drops can be observed, as the thumb does not participate in this test as much as the other fingers. The thumb essentially slides through the cylinder, which is why its load decrease is not visible in the plots. The thumb is the first to fail, followed by the little finger (first significant load drop), the index finger, the ring finger, and finally, the middle finger, which is the last to withstand the load. These are represented by trigger lines in the plots, and to maintain clarity, only the first trial's finger failures are represented.

Each time a fingers fails the load drastically decreases, then it rises but never returns to the level it had before the failure. This occurs because the wire loses tension during the process.

The smaller hand can withstand an average maximum load of approximately 0.9 kg, what corresponds to the point where the little finger fails. Analogously, the larger hand, can withstand an average maximum load of 1.5 kg. To validate the results of the pull test conducted on the small hand, a load test with the entire device was performed. This test consisted in the prosthesis holding a bag with 0.9 kg, in its three different elbow positions. The test was successful, demonstrating that the prosthesis was capable of holding the mass without failure in all tree positions. This assessment specifically focused on evaluating the resistance of the elbow region, since it was not evaluated during the pulling tests. Figure D.1 shows the test setup and results.

Additionally, these tests show a high level of noise, what might be mainly due to the wire being held by a person, which inevitably led to load variations. Regarding the small hand trials, there was a problem with one of them, which was only noticed afterwards, without the possibility to repeat it under the same conditions as before. As a result, only two trials are shown in the plot.

5.2.2 Grasp Type Tests

Different objects require distinct grasp types, and both prosthetic hands were tested to determine which types they support. Table 5.1 shows the results of grasp type tests performed on the small hand. From these results, it can be concluded that this prosthesis demonstrates to have a power grasp, of cylindrical type for small diameters (up to 15 mm) and for large diameters (up to 45 mm), and of disk type (up to 50 mm of diameter and 10 mm of thickness). Additionally, it has a precision grasp of inferior pincer type, limited to small objects. The other types of grasps failed. It is important to note that the prosthetic hand has small dimensions, so it is limited in object sizes that can grab, as a eight-years-old hand is, and rough and light materials adhere better. The hand span is approximately (112.0 ± 0.5) mm and the opening width between the thumb and index finger fingertips is approximately (93.0 ± 0.5) mm.

On a larger scale, the prosthetic hand showed some improved grasping capabilities for larger objects. The results of the grasp type tests performed to the larger hand are present in Table D.2. The cylindrical power grasp is effective for both small (up to 20 mm) and large diameters (up to 50 mm). Similarly, the disk-type power grasp is effective for objects up to 60 mm in diameter. With a hand span of (142.0 ± 0.5) mm and a opening width of (118.0 ± 0.5) mm, the larger hand offers greater finger movement and a wider opening compared to the smaller version. This suggests that the grasping capabilities are influenced by the dimensions of the terminal device. If it has a bigger surface area and opening width, it can grab objects of bigger dimensions and manipulate them better.

Given these results, along with the inability to maintain a grip, the prosthetic hand can

be used for hold objects temporarily, such as small bananas, small bottles, cookies, pens, pencils, rubbers and small toys. It is not designed to active use the objects it holds, but it provides support in certain activities. For example, it can hold a pen, but it can not write with it [48]. Therefore, despite its functionality may be limited, it can still be considered a functional terminal device. Additionally, children at this age commonly use bilateral activity (using both upper limb members) to carry objects of bigger dimensions, such as a ball or a larger bottle, and the prosthesis also supports this functionality. By promoting bilateral activity, the prosthesis not only enhances the child's ability to interact with their environment but also allows the development of motor skills and independence.

Table 5.1: Results of the grasp type tests performed on the small hand.

Grasp Classification	Grasp Type	Result
Power	Cylindrical Grasp (Large Diameter)	Yes (Up to 45 mm of diameter)
	Cylindrical Grasp (Small Diameter)	Yes (Up to 15 mm of diameter)
	Spherical Grasp	No
	Disk Grasp	Yes (Up to 50 mm of diameter and 10 mm of thickness)
Intermediate	Lateral Pinch	No
Precision	Tip Pinch	No
	Prismatic Finger	No
	Precision Disk	No
	Inferior Pincer	Yes (Limited to small sizes and certain shapes)

5.2.3 Goniometry

Goniometry was used to measure the joint angles in the prosthesis movements, and all the results are presented in Table D.1.

The device offers three distinct angle positions for elbow flexion: 29° (Position 1), 72° (Position 2), and 108° (Position 3). For shoulder medial rotation, it provides four positions: 13° (Position 2), 26° (Position 3), 42° (Position 4), 53° (Position 5). For shoulder external rotation, it provides three positions: 13° (Position 6), 23° (Position 7), 27° (Position 8). The neutral position is at 0° (Position 1).

Regarding the MP joints, the maximum flexion values are 63° for the thumb and between [73, 78]° for the other fingers, while standard human values are 55° for the thumb and 90° for the remaining fingers. For the proximal interphalangeal joints of the four fingers, the maximum flexion ranges from 61° to 84°, while the standard human maximum is 100°. Regarding thumb abduction, for palmar abduction, the thumb CMC joint is fixed at 46°, and for radial abduction, it is fixed at 74°. In a human hand, palmar abduction goes up to 45° and radial abduction goes up to 60°. From this results, the similarity with human hand motions can be noticed, since the reached angles are similar.

On the other hand, the distal interphalangeal joints of the four fingers and the interphalangeal joint of the thumb are fixed around 20°, which significantly differs from the human joints, which can flex up to 80°. This is the main reason of the poor grasping

capabilities of the developed device, as it restricts the types of grasps that can be performed and the variety of objects that can be securely held, since they can easily slip from the hand. Regarding hyperextension of the fingers, the device does not support it, since the maximum position the fingers reach is approximately 0° in all articulations. Since these results are not relevant they are not included in the table.

Systematic errors may arise from consistently mispositioning the goniometer. Random errors can arise from various sources, including incorrect positioning of the goniometer, incorrect reading of the measurements, and unwanted device movements due to instability in some components. Additionally, when the hand is closed, despite the efforts to remain it still, the wire might not be in the same pulled position and the whippletree mechanism might not distribute the force equally trough the five fingers throughout the all experiment, contributing to measurement variability. These errors can affect the precision of the results. For example, regarding elbow flexion, in Position 3, the prosthesis components exhibit greater stability due to the configuration of the forearm and elbow, resulting in higher precision in the measurements. In the remaining two positions, the presence of air gaps leads to more variable and less precise measurements.

5.2.4 Finite Element Analysis

In this study, FEA was performed to simulate load lifting and determine the best material for the finger "Hinges". Figure 5.8 shows the analysis conducted on the index finger with hinges made of TPU 98A. This simulation is also representative of the other four fingers, as they share similar geometry and dimensions.

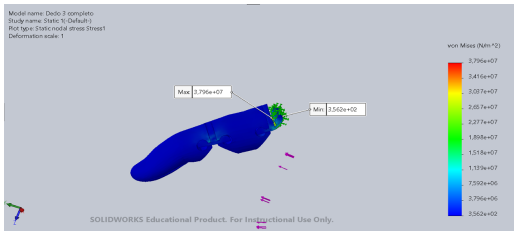

(a) Stress distribution.

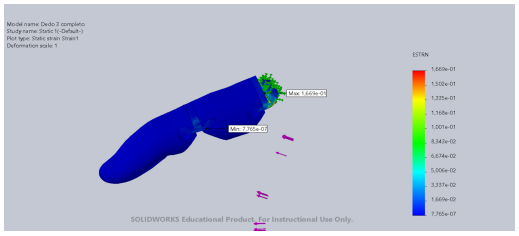

(b) Strain distribution.

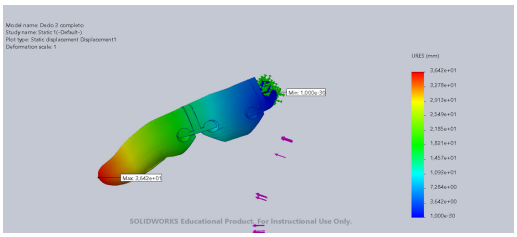

(c) Displacement distribution.

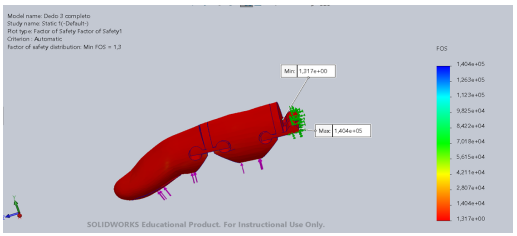

(d) Factor of safety distribution.

Figure 5.8: Finite element analysis of the index finger with hinges made of TPU 98A.

A maximum stress of $3.80 \times 10^7\ N/m^2$ resulted in a minimum safety factor of 1.32, ensuring its mechanical integrity. The maximum displacement suffered by the finger was 36.42 mm. The maximum strain was 0.17.

The most critical areas are the hinges and the surrounding regions, as they experience higher stress and strain levels. Since the hinges revealed as the most critical areas, other materials (Filaflex 82A and 95A) were studied besides TPU 98A, to see if there would be an improvement in hand resistance and performance. The results are shown in figures D.2 and D.3. For the same load (5N), for the Filaflex 95A, a maximum stress of 2.74×10^7 N/m^2 resulted in a minimum safety factor of 2.00. The maximum displacement suffered by the finger was 56.16 mm. The strain was 0.22. Analogously, for the Filaflex 82A, a maximum stress of 1.28×10^7 N/m^2 resulted in a minimum safety factor of 4.40. The maximum displacement suffered by the finger was 59.64 mm. The strain was 0.23.

Filaflex 82A was proved to be the most resistant material for hinges among those three, according to stress and FOS values and it allowed for a greater movement of the fingers, as stated by C. Patrão [50]. Nevertheless, the higher displacement and strain suffered result in a decreased capacity in grasping and to a decrease in the maximum pulling force (load) that the hand can withstand. Therefore, the most suitable choice is the TPU 98A, since it is the one that can provide a greater grasping force to the hand and allows the prosthesis to withstand a higher load, according to the values of strain and displacement suffered.

5.3 Product Evaluation

Figure 5.9 shows the case-study child wearing the device. To ensure a proper fit, the thermoforming technique was used on the "Arm Wrap" and "Shoulder Connector" to shape the child's shoulder. Additionally, EVA foam sheet was glued in critical areas inside the prosthesis to prevent discomfort or injury the child's limb. Straps were then placed around the child simulating an harness, and the cable was adjusted to her size. Once the prosthesis was properly fitted, the child was asked to perform the movements required to activate the cable mechanism. Initial difficulties were observed, which is understandable given that the child is not used to perform these movements and the responsible muscles are underdeveloped. A tendency to perform shoulder abduction instead of shoulder flexion was noted. However, after some practice, the child was able to execute the intended movements, and the hand successfully closed as the wire was pulled, as shown in Figure 5.9b. Six weaknesses of the device were found during this evaluation:

- The weight was identified as a concern by the child. However, this is common among congenital amputees, since they are not used to feel weight in that body part.
- The prosthetic arm was larger than the healthy one, which can be addressed by reducing the forearm length.
- The need for a way to replace the cable without disassembling the entire device. This can be solved by adding a new component that holds the cable at both ends. One possible location is in the grip locking mechanism place, since it does not work.

- The need for a new component to connect the "Shoulder Connector" to the harness straps, ensuring the device does not slip off the shoulder and stays in position. This issue was quickly addressed by adding an extra strap.
- The "Shoulder Connector", the "Scapula plate" and the "Clavicle plate" should be printed in TPU 98A. Although these components were not mentioned as pressure points by the case-study child, the "Shoulder Connector" did not fit perfectly on the shoulder area. Consequently, the use of TPU 98A is recommended as it allows for a better fit and increases the overall comfort of the device. After the case-study fitting, these TPU printings were tried and presented good results in one of the prototypes.
- The "Puller" should be printed in a more resistant material, such as PETG. During the explanation of the prosthesis mechanisms this component broke, but an additional one had been printed and was it quickly replaced. The specific cause of the failure was not identified, since this had never occurred before and only the filament was different. Nevertheless, using a more resistant material may address this issue.

The prosthesis weights 400 g, which is a very good result, and makes it a lightweighted device. This value englobes the entire prosthesis, with both the 3D printed and the non-3D printed parts. According to D. Segura et al., transhumeral prosthesis weights range from 403 g for body-powered devices to 3450 g for electronic devices [70]. The estimated material cost is approximately 18.7 €, classifying it as a low-cost device. This estimate includes only material expenses and excludes operational costs. The cost of the 3D printed parts (including support materials) is estimated at 9.7 €, as detailed in Table D.3. The cost of the non-3D printed parts, including screws, bolts, nuts, a compression spring, cable revetment, polyester wire, and straps, is estimated to be around 9 €. The total printing time is estimated in 60 hours and 25 minutes and the assembly time is about 2 hours. The patient fitting is relative but it took near 2 hours in this specific case-study.

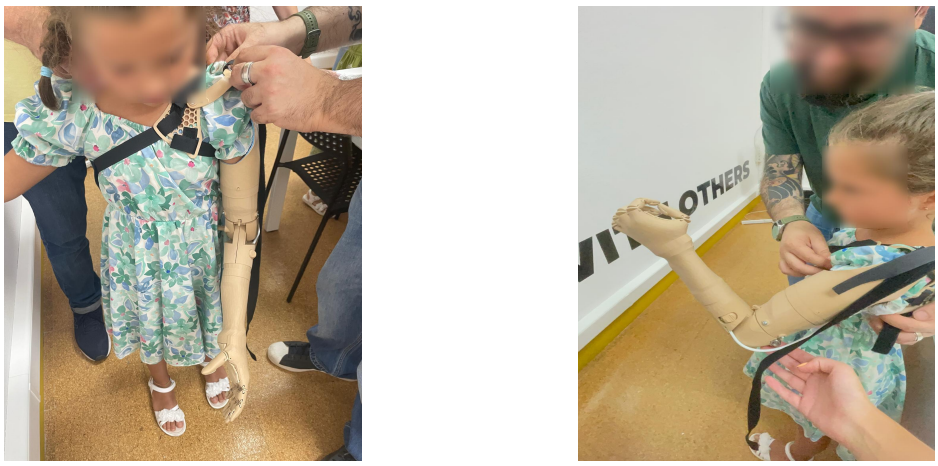

(a) Fitting of the prosthesis. (b) Prosthetic hand fully closed by the user.

Figure 5.9: Final prosthesis fitted on the case-study child.

6

Conclusion

This chapter summarizes the key achievements of the present study and offers suggestions for future work that could address the current device limitations and help creating a more complete device, along with the prosthesis evaluation results.

6.1 Study Achievements

Upper limb deformations can deeply impact a person's quality of life, making prosthetic rehabilitation essential for restoring function and enhancing independence. However, high rejection rates associated with the use of prosthetics remain a significant challenge, driven by factors such as weight, comfort, cost, and appearance.

While academia has made significant contributions to the field of prosthetics, there has been limited progress in developing body-powered hands with five moving fingers due to the complexity involved. As a result, simpler designs like hooks or hands with only a moving thumb are more common. Moreover, there is a gap in the development of body-powered transhumeral prostheses, due to its complexity in terms of DOFs. Finally, only a few of them manage to combat the key limitations presented above.

This work, with a 3D printed transhumeral body-powered prosthesis, aims to address these challenges and reduce rejection rates. It presents a comprehensive methodology for designing, printing, assembling, testing, and evaluating a transhumeral device. The iterative development process began with the *NIOP TH-S* model, which was continuously improved through several design modifications, leading to a final prototype. This final prototype was then validated through different tests and FEM analysis. Additionally, an adult-sized terminal device was created to allow for a more detailed study. Once the final prototype met the necessary criteria based on the tests results, the final product was developed, fitted to the case-study child and qualitatively evaluated.

The designed prosthesis solves the functional issues identified in the *NIOP TH-S* model, mainly concerning the hand. It has a more anthropomorphic design and closely matches the case-study child's skin tone, significantly improving its aesthetic appearance. It is composed by flexible materials in finger "Hinges", "Grips", "Palm Cover", "Shoulder

connector", "Scapula plate" and "Clavicle plate", what makes the device lighter and more comfortable. Therefore, the goal of substitute some rigid materials by flexible ones was also achieved. It is a low-cost (18.7 €) and a light-weighted (400 g) device, what shows the main advantages of the use of 3D printing in prosthetics, and makes the device particularly suitable for children, who require new prostheses frequently due to their rapid growth.

In terms of functionality, the device is activated by shoulder flexion and scapula abduction. It has twelve DOFs: one in the shoulder joints (allowing medial/external rotation of the shoulder), two in the elbow joints (allowing elbow flexion/extension and forearm supination/pronation) and nine in the finger joints (allowing fingers flexion/extension). The terminal device is a VC mechanism with five moving fingers that requires between 85.3 N and 163.2 N of activation cable force to fully close and it is capable of withstand loads up to at least 0.9 kg. Its main limitation is the grip locking system, that does not work, leading to the inability to maintain a constant grip and limited grasping capabilities.

In conclusion, this work adds a significant contribution to prosthetic rehabilitation, demonstrating the impact of 3D printing. The developed device was designed not only for the case-study child but also for any child with a similar transhumeral deficiency. Finally, this prosthesis combines functionality, although limited, with aesthetics, affordability, and comfort, which is a lacking combination in the transhumeral prosthetics market.

6.2 Future Work

There are several aspects that can be improved in order to enhance the device's functionality and aesthetics. Further work should include:

- **Introduction of flexible materials**: One of the goals that was not achieved in total was the incorporation of flexible materials into the device. Despite the finger "Hinges", "Grips", "Palm Cover", "Shoulder Connector, "Scapula plate" and "Clavicle plate" being made with flexible materials and benefit from its characteristics, the goal was to make the prosthesis more comfortable and lighter. So, a good future improvement would be the incorporation of flexible materials in the upper region of the device, that is in contact with the amputee's limb, avoiding the need to use foam sheet, that increases the temperature in the area and makes the device even heavier. Despite some attempts among the "Upper Arm Base" and the "Arm Wrap", this did not work, as the device would lose is functionality.

- **Improvement of the hand design**: Regarding hand joints, several improvements can be done. First, the distal interphalangeal joints and the thumb's interphalangeal joint should not be fixed. Additionally, all the joints should recede slightly. This is especially important for the MP joints, which are currently positioned incorrectly and extend beyond their real location. Furthermore, the thumb should be able to perform radial and palmar abductions, which means the thumb's CMC joint should be added to the device's DOFs. These modifications will improve grasping

capabilities and expand the range of object sizes that can be effectively grasped. Regarding the hand itself, it would benefit with the addition of a hole to become possible using a pen or cutlery. This would allow for the actual use of these objects, rather than just holding them, as the current prosthesis does. This feature is common among passive prostheses and it would enhance the functionality of the device for everyday tasks. The wrist design can also be improved, which could be achieved by 3D scanning a human wrist, as it was done for the forearm.

- **Improvement of the grip locking mechanism**: Regarding the grip locking mechanism, which should lock the hand grip position, it needs to be completely changed. The current mechanism is not strong enough, even with design modifications. This is the most critical issue to address, as a robust locking mechanism will significantly enhance the device's functionality, allowing it to securely hold objects and maintain a firm grip. One important thing to take into consideration while working on that is the drop in grasp force that occurs between the initiation of the grip and the activation of the locking mechanism [59].

- **Perform additional tests**: Grasping force is one of the most important characteristics to measure in terminal devices. Typically, it is measured with force or pressure sensors, placed on an object's surface. The object is then grasped and the maximum force applied in the object is measured [59–61]. Alternatively, a dynamometer can also be used. Additionally, FEA could be used to simulate the traction force generated by the control cable [55]. It could also be used to study different prosthesis' components besides the fingers, such as the components of the "Elbow" and "Shoulder" sections. These are complementary tests that can be done during the product validation phase.

- **Improvement of the force transmission**: Despite the activation cable force required to fully close the terminal device being within the range of commercially available prostheses and the case-study child was able to achieve it, there is still room for improvement. To improve force transmission from the shoulder region to the terminal device, a pulley system could be implemented along the prosthesis instead of the current direct transmission method. This system would require a large and a small pulley. The large pulley will be positioned near the shoulder section, while the smaller pulley will be positioned near the terminal device. When the user flexes the shoulder to activate the prosthesis, the control cable moves through the large fixed pulley and then through the small movable pulley. The smaller pulley moves faster due to its smaller radius, resulting in a quicker and more efficient movement of the terminal device, with less amplitude of shoulder flexion. This setup reduces the required force, improving functionality [57].

While challenges remain, this work represents a step forward in improving the quality of life for those with upper limb deficiencies.

Bibliography

[1] J. M. Lourenço. *The NOVAthesis LaTeX Template User's Manual*. NOVA University Lisbon. 2021. URL: https://github.com/joaomlourenco/novathesis/raw/main/template.pdf (cit. on p. i).

[2] e-NABLE. *Enabling The Future*. URL: https://enablingthefuture.org/?gclid=Cj0KCQiAn-2tBhDVARIsAGmStVnjHJWiQKdbw3prw3m1xtyPijEj00wD1WRoBjoBylrVRHX8V7hNI4MaAk6YEALw_wcB (cit. on pp. 1, 12, 52, 54).

[3] Ottobock. "Website". In: (). URL: https://www.ottobock.com/en-us/home (cit. on pp. 2, 8, 9, 51).

[4] A. S. f. S. of the Hand. *Upper limb joints*. URL: https://www.assh.org/handcareprod/safety/joints (cit. on pp. 3, 4).

[5] G.O.Philips. "The Scientific Basis of Tissue Transplantation". In: *The Scientific Basis of Tissue Transplantation*. Ed. by A. Nather. Woorld Scientific. Chap. Anatomy of. URL: https://books.google.pt/books?hl=pt-PT&lr=&id=-tIywX9QXmQC&oi=fnd&pg=PA3&dq=upper+limb+anatomy+&ots=wKM5JI3VFR&sig=vnllvR4gt6EDQ5tLhgmvvKapabE&redir_esc=y#v=onepage&q=upper%20limb%20anatomy&f=false (cit. on p. 3).

[6] S. Tenim. "DESIGN OF AN AFFORDABLE ANTHROPOMORPHIC MECHANICAL PROSTHETIC HAND". PhD thesis. 2014 (cit. on pp. 3, 4).

[7] U. K. Latif et al. "Designing for Rehabilitation Movement Recognition and Measurement in Virtual Reality". In: *Proceedings of the Design Society* 3.JULY (2023), pp. 1387–1396. ISSN: 2732527X. DOI: 10.1017/pds.2023.139 (cit. on pp. 3, 49).

[8] C. L. TAYLOR. "The biomechanics of control in upper-extremity prostheses." In: *Artificial limbs* 2.3 (1955), pp. 4–25. ISSN: 00043729 (cit. on pp. 3, 4, 49).

[9] T. Feix et al. "The GRASP Taxonomy of Human Grasp Types". In: *IEEE Transactions on Human-Machine Systems* 46.1 (2016), pp. 66–77. ISSN: 21682291. DOI: 10.1109/THMS.2015.2470657 (cit. on pp. 4, 5).

[10] C. C. Lien. "A scalable model-based hand posture analysis system". In: *Machine Vision and Applications* 16.3 (2005), pp. 157–169. ISSN: 09328092. DOI: 10.1007/s00138-004-0167-0 (cit. on p. 4).

[11] Z. Deng and J. Zhang. "Learning Synergies-based In-hand Manipulation with Reward Shaping". In: *CAAI Transactions on Intelligence Technology* 5 (2020-07). DOI: 10.1049/trit.2019.0094 (cit. on p. 4).

[12] S. M. Tayel et al. "A morpho-etiological description of congenital limb anomalies". In: *Annals of Saudi Medicine* 25.3 (2005), pp. 219–227. ISSN: 02564947. DOI: 10.5144/0256-4947.2005.219 (cit. on p. 5).

[13] J. T. Le and P. R. Scott-Wyard. "Pediatric Limb Differences and Amputations". In: *Physical Medicine and Rehabilitation Clinics of North America* 26.1 (2015), pp. 95–108. ISSN: 15581381. DOI: 10.1016/j.pmr.2014.09.006. URL: http://dx.doi.org/10.1016/j.pmr.2014.09.006 (cit. on p. 5).

[14] N. B. Gold, M. N. Westgate, and L. B. Holmes. "Anatomic and etiological classification of congenital limb deficiencies". In: *American Journal of Medical Genetics, Part A* 155.6 (2011), pp. 1225–1235. ISSN: 15524825. DOI: 10.1002/ajmg.a.33999 (cit. on p. 5).

[15] R. Palisano, M. Orlin, and J. Schreiber. *Campbell's Physical Therapy for Children Expert Consult*. URL: https://books.google.pt/books?hl=pt-PT&lr=&id=ruJgDwAAQBAJ&oi=fnd&pg=PA272&dq=acquired+limb+deficiencies+amputations&ots=Ap8Pdue_61&sig=VtboHVgj9awDJ0XWGkw0GyxI8h8&redir_esc=y#v=onepage&q=acquired%20limb%20deficiencies%20amputations&f=false (cit. on p. 5).

[16] V. Lopes. "Design and Development of an Upper Limb Prosthesis". In: June (2017), p. 11 (cit. on pp. 5, 13, 14).

[17] F. Cordella et al. "Literature review on needs of upper limb prosthesis users". In: *Frontiers in Neuroscience* 10.MAY (2016), pp. 1–14. ISSN: 1662453X. DOI: 10.3389/fnins.2016.00209 (cit. on pp. 5, 49).

[18] D. Services and W. Hospital. "Iso/ispo". In: Table 1 (1991), pp. 67–69 (cit. on pp. 5, 49).

[19] I. Y. H. Ng et al. "NIH Public Access". In: *J Neurochem* 4.1 (2015), pp. 1–15. ISSN: 15378276. DOI: 10.1097/PHM.0b013e3181b306ec.Chronic (cit. on p. 5).

[20] H. Burger and G. Vidmar. "A survey of overuse problems in patients with acquired or congenital upper limb deficiency". In: *Prosthetics and Orthotics International* 40.4 (2016), pp. 497–502. ISSN: 17461553. DOI: 10.1177/0309364615584658 (cit. on pp. 5, 11).

[21] M. A. Kuyper et al. "Prosthetic management of children in the Netherlands with upper limb deficiencies". In: *Prosthetics and Orthotics International* 25.3 (2001), pp. 228–234. ISSN: 03093646. DOI: 10.1080/03093640108726606 (cit. on p. 6).

[22] K. Yiğiter et al. "Demography and function of children with limb loss". In: *Prosthetics and Orthotics International* 29.2 (2005), pp. 131–138. ISSN: 03093646. DOI: 10.1080/03093640500199703 (cit. on p. 6).

[23] T. J. Gordelier et al. "Optimising the FDM additive manufacturing process to achieve maximum tensile strength: a state-of-the-art review". In: *Rapid Prototyping Journal* 25.6 (2019), pp. 953–971. ISSN: 13552546. DOI: 10.1108/RPJ-07-2018-0183 (cit. on p. 6).

[24] H. I. Medellin-Castillo and J. Zaragoza-Siqueiros. "Design and Manufacturing Strategies for Fused Deposition Modelling in Additive Manufacturing: A Review". In: *Chinese Journal of Mechanical Engineering (English Edition)* 32.1 (2019). ISSN: 21928258. DOI: 10.1186/s10033-019-0368-0. URL: https://doi.org/10.1186/s10033-019-0368-0 (cit. on p. 6).

[25] H. Agrawaal and J. E. Thompson. "Additive manufacturing (3D printing) for analytical chemistry". In: *Talanta Open* 3.February (2021), p. 100036. ISSN: 26668319. DOI: 10.1016/j.talo.2021.100036. URL: https://doi.org/10.1016/j.talo.2021.100036 (cit. on p. 6).

[26] Protolabs Network by Hubs. *3D printing*. URL: https://www.hubs.com/knowledge-base/ (cit. on pp. 6, 7).

[27] All3DP. *3D printing materials price*. URL: https://all3dp.com/2/3d-printer-material-cost-the-real-cost-of-3d-printing-materials/ (cit. on p. 6).

[28] Recreus. *Filaflex*. URL: https://recreus.com/gb/content/35-filaflex (cit. on p. 7).

[29] NinjaTek. *Ninjaflex*. URL: https://ninjatek.com/shop/ninjaflex/ (cit. on p. 7).

[30] J. Prusa. *3D Printing Handbook (User Manual)* (cit. on p. 7).

[31] PRUSA Research by Josef Prusa. *Help Prusa*. URL: https://help.prusa3d.com/article/layers-and-perimeters_1748 (cit. on p. 7).

[32] Arm Dynamics. *Prosthetic Options*. URL: https://www.armdynamics.com/our-care/prosthetic-options (cit. on pp. 8, 9, 51).

[33] L. Trent et al. "A narrative review: current upper limb prosthetic options and design". In: *Disability and Rehabilitation: Assistive Technology* 15.6 (2020), pp. 604–613. ISSN: 17483115. DOI: 10.1080/17483107.2019.1594403 (cit. on pp. 8, 11).

[34] S. Hussain, S. Shams, and S. Jawaid Khan. "Impact of Medical Advancement: Prostheses". In: *Computer Architecture in Industrial, Biomechanical and Biomedical Engineering* November (2019). DOI: 10.5772/intechopen.86602 (cit. on pp. 8, 9).

[35] J. I. Efanov et al. "A review of utilities and costs of treating upper extremity amputations with vascularized composite allotransplantation versus myoelectric prostheses in Canada". In: *JPRAS Open* 32 (2022), pp. 150–160. ISSN: 23525878. DOI: 10.1016/j.jpra.2022.03.003. URL: https://doi.org/10.1016/j.jpra.2022.03.003 (cit. on p. 8).

[36] J. Uellendahl. "Myoelectric versus Body-Powered Upper-Limb Prostheses: A Clinical Perspective". In: *Journal of Prosthetics and Orthotics* 29.4 (2017), P25–P29. ISSN: 10408800. DOI: 10.1097/JPO.0000000000000151 (cit. on pp. 8, 11).

[37] Steeper Group. *Steeper*. URL: https://www.steepergroup.com/ (cit. on pp. 9, 51).

[38] M. J. Hall et al. "Essentials of Pediatric Prosthetics". In: *Journal of the Pediatric Orthopaedic Society of North America* 2.3 (2020), p. 168. ISSN: 27682765. DOI: 10.55275/jposna-2020-168 (cit. on p. 9).

[39] M. Kutz. *Biomedical Engineering and Design Handbook*. Vol. 2. 2009, pp. 537–598. ISBN: 9780071704748 (cit. on pp. 9, 10).

[40] J. Shaperman et al. "Is body powered operation of upper limb prostheses feasible for young limb deficient children?" In: *Prosthetics and Orthotics International* 19.3 (1995), pp. 165–175. ISSN: 17461553. DOI: 10.3109/03093649509168000 (cit. on p. 9).

[41] N. Nikafrooz and A. Leonessa. "A single-actuated, cable-driven, and self-contained robotic hand designed for adaptive grasps". In: *Robotics* 10.4 (2021). ISSN: 22186581. DOI: 10.3390/robotics10040109 (cit. on p. 10).

[42] "Design Process of Whippletree-Like Mechanism for Versatile Gripping in Arm Prosthesis". In: *Lecture Notes in Mechanical Engineering* October (2023), pp. 485–494. ISSN: 21954364. DOI: 10.1007/978-981-99-1245-2_45 (cit. on p. 10).

[43] A. Satriawan et al. "Karla: A Simple and Affordable 3-D Printed Body-Powered Prosthetic Hand with Versatile Gripping Technology". In: *Designs* 7.2 (2023), pp. 1–15. ISSN: 24119660. DOI: 10.3390/designs7020037 (cit. on pp. 10, 52).

[44] J. S. Cuellar et al. "Ten guidelines for the design of non-assembly mechanisms: The case of 3D-printed prosthetic hands". In: *Proceedings of the Institution of Mechanical Engineers, Part H: Journal of Engineering in Medicine* 232.9 (2018), pp. 962–971. ISSN: 20413033. DOI: 10.1177/0954411918794734 (cit. on p. 10).

[45] E. Biddiss and T. Chau. "Upper limb prosthesis use and abandonment: A survey of the last 25 years". In: *Prosthetics and Orthotics International* 31.3 (2007), pp. 236–257. ISSN: 03093646. DOI: 10.1080/03093640600994581 (cit. on p. 11).

[46] S. Salminger et al. "Current rates of prosthetic usage in upper-limb amputees–have innovations had an impact on device acceptance?" In: *Disability and Rehabilitation* 44.14 (2022), pp. 3708–3713. ISSN: 14645165. DOI: 10.1080/09638288.2020.1866684. URL: https://doi.org/10.1080/09638288.2020.1866684 (cit. on p. 11).

[47] N. Jarrassé et al. "Phantom-mobility-based prosthesis control in transhumeral amputees without surgical reinnervation: A preliminary study". In: *Frontiers in Bioengineering and Biotechnology* 6.NOV (2018), pp. 1–14. ISSN: 22964185. DOI: 10.3389/fbioe.2018.00164 (cit. on p. 11).

[48] S. D. Dunnen. "The design of an adaptive finger mechanism for a hand prosthesis". In: *TU Delft* (2009). ISSN: 0094114X (cit. on pp. 11, 34).

[49] e-NABLE. "NIOP TH-S". In: (). URL: https://www.thingiverse.com/thing:4884632/files (cit. on pp. 12, 16, 21, 54, 56).

[50] C. Patrão. "DEVELOPMENT AND OPTIMIZATION OF A LOW-COST MYOELECTRIC TRANSHUMERAL PROSTHESIS". In: (2024) (cit. on pp. 12–14, 16, 17, 20, 36, 49, 50, 55, 56).

[51] E-NABLE. *Kinetic Hand*. URL: https://www.thingiverse.com/thing:4618922 (cit. on pp. 13, 21, 54).

[52] R. Herbert, J. W. Jeong, and W. H. Yeo. "Soft material-enabled electronics for medicine, healthcare, and human-machine interfaces". In: *Materials* 13.3 (2020), pp. 2–5. ISSN: 19961944. DOI: 10.3390/ma13030517 (cit. on p. 13).

[53] A. Oliveira, C. Quaresma, and B. Soares. "Development of a 3D-printed body-powered prosthesis with flexible materials". In: *Advances and Current Trends in Biomechanics* (2021), pp. 294–298. DOI: 10.1201/9781003217152-65 (cit. on pp. 13, 21, 29, 54, 57, 59).

[54] F. C. B. Dias Pinheiro. "Development of a Functional Upper Limb Prosthesis". In: May (2018), p. 8 (cit. on pp. 13, 14).

[55] M. M. Kusters. "A 3D printed transhumeral arm prosthesis". In: (2020), pp. 1–29 (cit. on pp. 14, 40, 54, 62).

[56] Simplify3D. *PVA*. URL: https://www.simplify3d.com/resources/materials-guide/pva/ (cit. on p. 14).

[57] G. K. Jones and R. Stopforth. "Mechanical Design and Development of the Touch Hand II Prosthetic Hand". In: *Journal of the South African Institution of Mechanical Engineering* 32.January (2016), pp. 23–34. URL: http://www.saimeche.org.za (cit. on pp. 14, 25, 40, 54).

[58] K. T. Ulrich and Steven D. Eppinger. *Product design and development*. 2012. ISBN: 9780073404776. DOI: 10.1016/0956-5663(92)90013-D (cit. on p. 15).

[59] G. Smit and D. H. Plettenburg. "Efficiency of voluntary closing hand and hook prostheses". In: *Prosthetics and Orthotics International* 34.4 (2010), pp. 411–427. ISSN: 03093646. DOI: 10.3109/03093646.2010.486390 (cit. on pp. 21, 32, 40).

[60] R. Mio, M. Sánchez, and Q. Valverde. "Mechanical testing methods for body-powered upper-limb prostheses: A review". In: *Proceedings - 2018 IEEE 18th International Conference on Bioinformatics and Bioengineering, BIBE 2018* November (2018), pp. 170–176. DOI: 10.1109/BIBE.2018.00040 (cit. on pp. 21, 32, 40).

[61] R. Mio et al. "Mechanical testing methods for body-powered upper-limb prostheses: A case study". In: *Advances in Science, Technology and Engineering Systems* 4.5 (2019), pp. 61–68. ISSN: 24156698. DOI: 10.25046/aj040508 (cit. on pp. 21, 32, 40).

[62] A. G. em Saúde. "Manual De Goniometria Medição Dos Ângulos". In: *Gestão em Saúde* (2000). URL: http://acegs.com.br/wp-content/uploads/2016/06/MANUAL-DE-GONIOMETRIA-FINAL.pdf (cit. on p. 24).

[63] C. Conrad. *Adding PLA as a costum material in Fusion*. URL: https://www.youtube.com/watch?v=OoS_lBgmtTo&t=172s (cit. on pp. 25, 61).

[64] BCN3D Filaments. "BCN3D Filaments". In: (). URL: https://www.bcn3d.com/wp-content/uploads/2023/01/BCN3D-Filaments-Technical-Data-Sheet-TPU-98A.pdf (cit. on pp. 25, 61).

[65] Filament2print. *Filament2print*. URL: https://filament2print.com/gb/flexible-tpe-tpu/1288-reciflex.html (cit. on pp. 25, 61).

[66] L. Rodríguez-Parada, S. De La Rosa, and P. F. Mayuet. "Influence of 3D-printed TPU properties for the design of elastic products". In: *Polymers* 13.15 (2021). ISSN: 20734360. DOI: 10.3390/polym13152519 (cit. on pp. 25, 61).

[67] Filament2print. *filament2print Filaflex 95A*. URL: https://filament2print.com/gb/flexible-tpe-tpu/1750-filaflex-tpu-95a.html (cit. on pp. 25, 61).

[68] A. L. N. Joseacute et al. "Structural numerical analysis of a three fingers prosthetic hand prototype". In: *International Journal of Physical Sciences* 8.13 (2013), pp. 526–536. DOI: 10.5897/ijps2013.3824 (cit. on p. 25).

[69] M. N. A. Mohd Nor et al. "Simulation and performance evaluation of a new type of powered dynamic ankle foot orthosis". In: *2011 IEEE Colloquium on Humanities, Science and Engineering, CHUSER 2011* Chuser (2011), pp. 167–171. DOI: 10.1109/CHUSER.2011.6163709 (cit. on p. 25).

[70] D. Segura et al. "Upper Limb Prostheses by the Level of Amputation : A Systematic Review". In: (2024), pp. 277–300 (cit. on p. 37).

[71] M. Mancuso. "Evaluation and robotic simulation of the glenohumeral joint". In: June (2020) (cit. on p. 48).

[72] Wikimedia. *Upper Limb Anatomy*. URL: https://upload.wikimedia.org/wikipedia/commons/4/49/Human_arm_bones_diagram.svg (cit. on p. 48).

[73] J. M. d. S. A. C. A. J. S. C. Z. J. E. P. O. V. Tavares. *Anatomia Geral Moreno*. 6ª. 2011 (cit. on p. 50).

[74] A. prosthetics. *APC prosthetics*. URL: https://apcprosthetics.com.au/ (cit. on p. 51).

[75] K. P. L. Kumarage et al. "A novel 3 -D printed wrist powered upper limb prosthesis using whippletree mechanism". In: (2019), pp. 661–666 (cit. on p. 52).

[76] D. Esposito et al. "The "federica" hand". In: *Bioengineering* 8.9 (2021), pp. 1–21. ISSN: 23065354. DOI: 10.3390/bioengineering8090128 (cit. on p. 52).

[77] H. Khazri et al. "Hand Anthropometry: Baseline Data of The Major Ethnic Groups in Sabah". In: *Borneo Journal of Medical Sciences (BJMS)* 17.1 (2023). ISSN: 1985-1758. DOI: 10.51200/bjms.v17i1.3780 (cit. on p. 61).

A

Complementary information on the Theoretical Concepts

This appendix focus on the upper body anatomy, giving additional information on bones, joints, muscles and body movements considered relevant for the understanding of this study. It also provides information on upper limb deficiencies and amputations. Additionally, it contains examples of commercially available transhumeral prostheses of different types and whippletree mechanisms used in prosthetic hands.

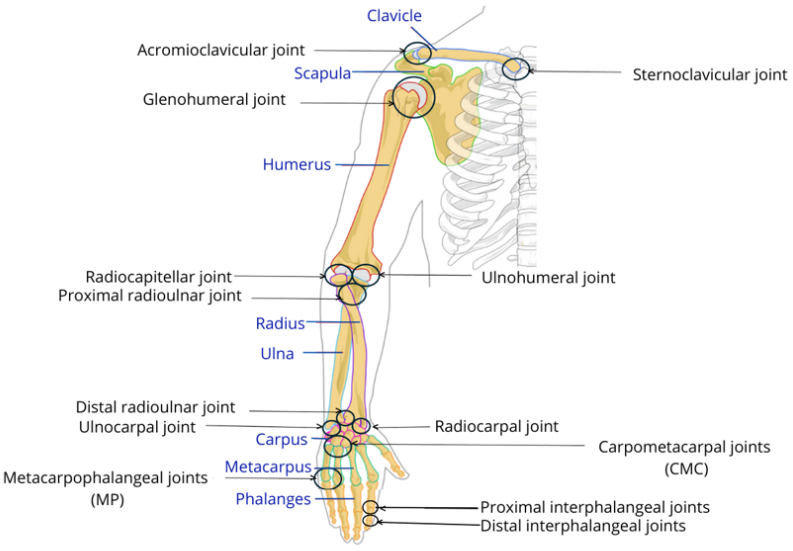

Figure A.1: Upper limb bones and joints. Adapted from [71] and [72].

Table A.1: Upper limb movements considered relevant for this work [7, 8]. Adapted from [50].

Region	Motion	Description
Shoulder girdle	Elevation	Moving the scapula superiorly in the frontal plane
	Depression	Moving the scapula inferiorly in the frontal plane
	Protraction	Moving the scapula anteriorly in the transverse plane
	Retraction	Moving the scapula posteriorly in the transverse plane
Shoulder	Flexion	Anterior movement of the arm in the sagittal plane
	Extension	Posterior movement of the arm in the sagittal plane
	Internal Rotation	Rotating the arm medially
	External Rotation	Rotating the arm laterally
	Abduction	Moving the arm away from the body in the frontal plane
	Adduction	Moving the arm towards the body in the frontal plane
Elbow	Flexion	Decreasing the angle between the forearm and the upper arm
	Extension	Increasing the angle between the forearm and the upper arm
	Pronation	Rotating the forearm medially in the transverse plane
	Supination	Rotating the forearm laterally in the transverse plane
Wrist	Flexion	Bending the wrist
	Extension	Straightening the wrist
	Ulnar Deviation	Moving the wrist towards the little finger in the frontal plane
	Radial Deviation	Moving the wrist towards the thumb in the frontal plane
Fingers	Flexion	Bending the fingers
	Extension	Straightening the fingers
	Abduction	Moving the fingers away in the frontal plane
	Adduction	Moving the fingers closer in the frontal plane

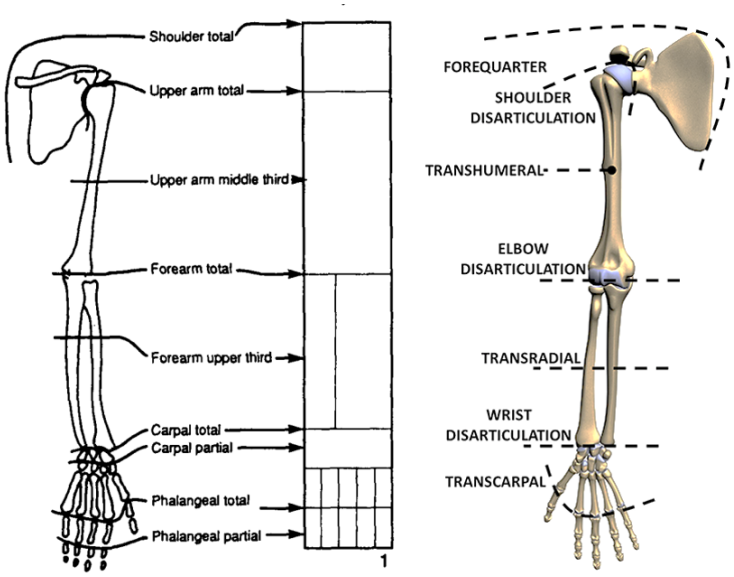

Figure A.2: Upper limb deficiencies and corresponding amputation designations[17, 18].

Table A.2: Upper limb muscles considered relevant for this work [73]. Adapted from [50].

Muscle	Origin	Insertion	Group
Trapezius	Superior nucal line, external occipital protuberance, spinous process of C7 and T1-T10 vertebrae	Lateral third of clavicle, acromium, and posterior spine of scapula	Shoulder
Deltoid	Lateral third of anterior clavicle, acromium, inferior edge of spine of scapula	Deltoid tuberosity of humerous	Back
Latissimus dorsi	Spinous process of T7-L5 vertebrae, external side of iliac crest, sacred crest and last 3 ribs	Inrertubercular sulcus of humerous	Back
Rhomboid major	Spinous process of T2-T5	Medial region of scapula	Back
Rhomboid minor	Spinous process of C7 and T1 vertebrae	Medial region of scapula	Back
Pectoralis major	Medial third of clavicle, sternum, 6 first costal cartilages	Lateral lip of intertubercular sulcus	Chest
Pectoralis minor	Outer surface of ribs 3-5	Coracoid process of scapula	Chest
Biceps	Long head: supraglenoid tubercle of scapula; Short head: coracoid process	Radial tuberosity	Arm
Triceps	Long head: infraglenoid cavity of scapula; Lateral head: upper half of posterior humerus; Medial head: upper half of anterior humerus	Olecranon	Arm
Coracobrachialis	Coracoid process	Medial surface of the humerous	Arm

Table A.3: Examples of commercialized transhumeral prostheses.

Type	Manufacturer	Model	
Passive	©Steeper		[37]
Externally-Powered	©Ottobock		[3]
Body-Powered	©APC Prosthetics		[74]
Hybrid	©Arm Dynamics	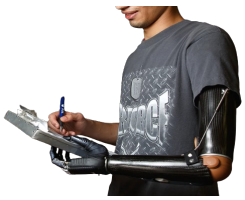	[32]

Table A.4: Examples of whippletree mechanisms.

Description	Designer	Design	
2D ring shaped mechanism.	Kumarage et al.	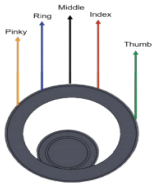	[75]
2D half circular ring shaped mechanism.	Kumarage et al.		[75]
3D pin-based mechanism.	Trusaji et al.	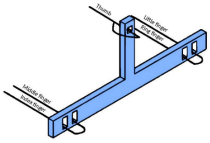	[43]
"Karla Hand" 3D triangle shaped mechanism.	Trusaji et al.	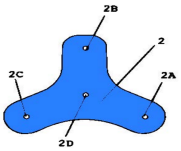	[43]
"Kinetic Hand" 2D pin-based mechanism.	e-NABLE	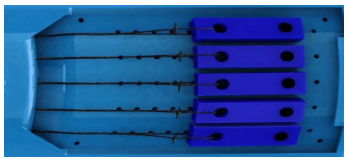	[2]
"Frederica Hand" 2D multi-pulley mechanism.	Esposito et al.	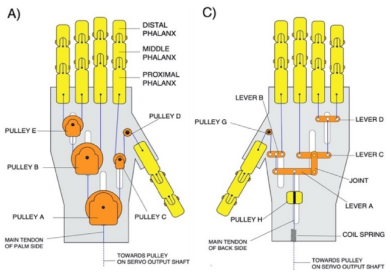	[76]

B

Complementary information on the State of the Art

This appendix contains examples of existing 3D printed devices that inspired this work, previously described on Chapter 3. It begins with three examples of e-NABLE prostheses, followed by a prosthesis made with flexible materials, and concludes with two prostheses made solely with rigid materials.

Table B.1: 3D printed prostheses.

Model Name	Designer	Design	
NIOP TH-S	e-NABLE	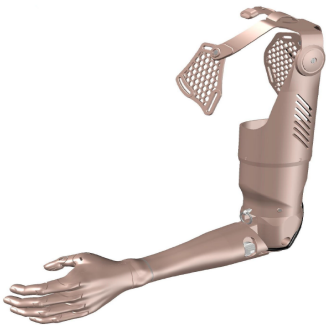	[49]
Kinetic Hand	e-NABLE		[51]
-	e-NABLE		[2]
-	Ana Oliveira		[53]
ARM3D	Madelon M.A. Kusters	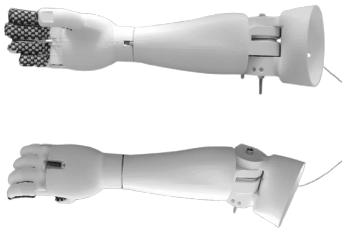	[55]
Touch Hand II	R. Stopforth et al.		[57]

C

Complementary information on the Methodology

This appendix provides complementary information on Chapter 4. It provides insights on the *NIOP TH-S* prosthesis, including its components, the scaling parameters used on *OpenScad* software and the first measurements of the case-study child taken by Catarina Patrão [50]. Additionally, it shows the mold used for thermoforming the "Arm Wrap" part. It also provides a detailed description on the new measurements collection, with a guide that explains how these were collected and the resultant measurements. It contains additional information on printing, showing the printing parameters used in Filaflex 82A printings. It also includes details of the mechanical tests that were performed, showing the workstation setup for each test and the support fixtures that were used. A visual representation of hand span and hand opening width measurements is also presented. Finally, additional details on the methodology of FEA are provided, with the properties of the studied materials.

C.1 *NIOP TH-S*

Table C.1: Selected parameters on *OpenScad* Software.

Parameter	**Selected Option**
Padding Thickness	2mm
Driveline	yes
Forearm cover	No
Wrist Attach Option	NIOP Wrist

Table C.2: Measurements of the case-study child taken by Catarina Patrão. Adapted from [50].

Feature	Dimension (mm)
Upper Arm Length	180
Bicep Circumference	150
Forearm Circumference	170
Forearm Length	180

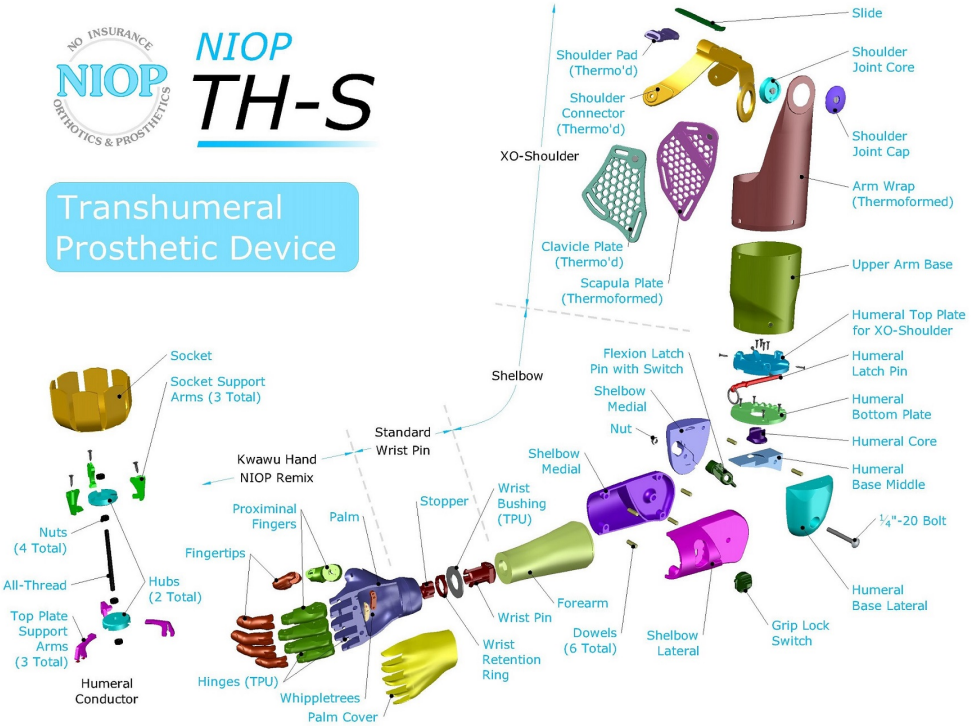

Figure C.1: Components of the e-NABLE prosthesis *NIOP TH-S* [49].

C.2 Design

Figure C.2: Mold used to thermoform the "Arm Wrap"

C.3 Measurements assessment procedure

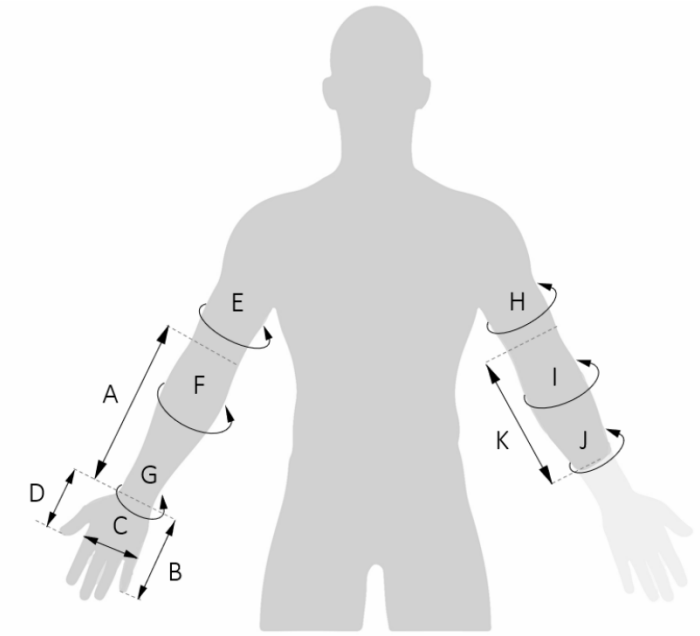

Figure C.3: Measurements guide, adapted to a transhumeral amputation. Measurements H, I, and J correspond to the top, middle, and bottom of the amputated limb, respectively. K measurement goes from the armpit to the end of the stump [53].

Table C.3: Measurements of the case-study patient.

Measurement	**Value in mm**
A	185
B	90
C	75
D	85
E	210
F	175
G	125
H	210
I	185
J	120
K	160

C.4 Printing

Table C.4: Printing parameters used in Filaflex 82A printings, based on set b6 found by Ana Oliveira. "(x)" means that the parameter is selected. "(-)" means that the parameter is disabled. Adapted from [53].

Category	Parameter	Property	Value
Print	**Layers and Perimeters**	Vertical shells (Perimeters) (mm)	2
		Detect Thin walls	-
	Infill	Fill density (%)	15
	Support Material	Style	Organic
	Speed	Perimeters (mm/s)	15
		Small Perimeters (mm/s)	15
		External Perimeters (mm/s)	15
		Top Solid Infill (mm/s)	15
		Solid Infill (mm/s)	15
		Support Material (mm/s)	15
		Bridges (mm/s)	15
		Gap fill (mm/s)	15
Filament	**Filament**	Extrusion Multiplier	1.25
		Temperature (Bed) (°C)	0
	Filament Overrides	Retraction length (mm)	3.5
		Lift height (mm)	0.04
		Only lift z above (mm)	0
		Only lift z below (mm)	209
		Retraction speed (mm/s)	35
		Deretraction speed (mm/s)	35
		Deretraction extra length (mm)	0
		Minimum travel after retraction (mm)	1
		Retract on layer change	x
		Wipe while retracting	x
		Retract amount before wipe (%)	0
Printer	**Extruder**	Retraction length (mm)	3.5
		Lift height (mm)	0.04
		Deretraction speed (mm/s)	35

C.5 Mechanical Tests

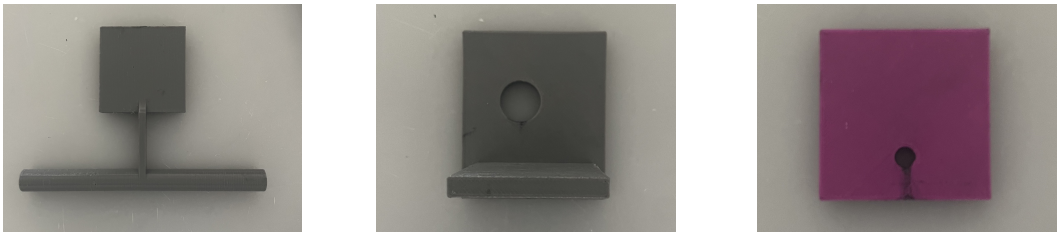

(a) 1o mm cylinder support. (b) Hand support. (c) Cable support.

Figure C.4: Support fixtures.

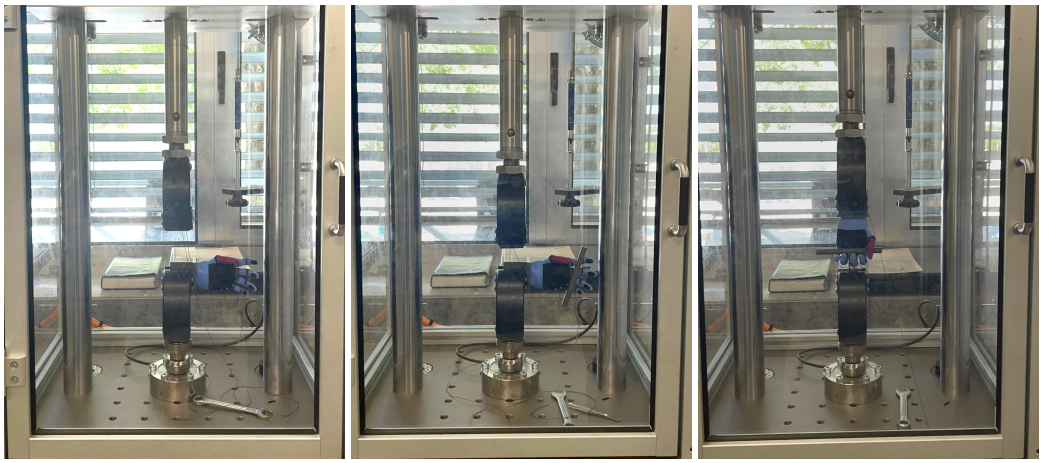

(a) Close test initial position. (b) Grasp test initial position. (c) Pull test initial position.

Figure C.5: Mechanical testes performed to the small hand.

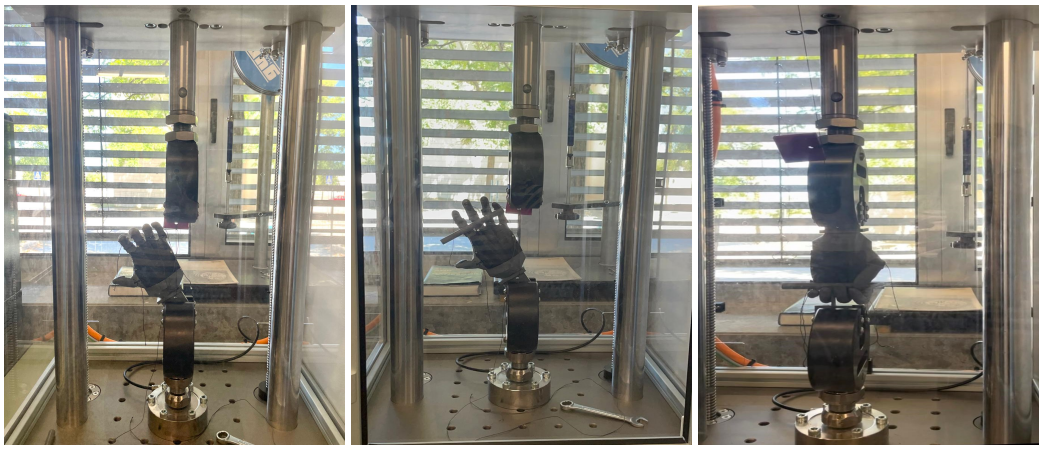

(a) Close test initial position. (b) Grasp test initial position. (c) Pull test initial position.

Figure C.6: Mechanical testes performed to the larger hand.

C.6 Grasp Type Tests

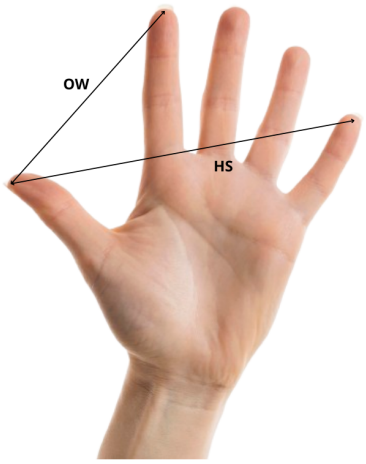

Figure C.7: Representation of hand span (HS) and opening width between the thumb and the index finger (OW). Adapted from [77].

C.7 Finite Element Analysis

Table C.5: Properties of the studied materials [63–67].

Material Property	PLA	TPU 98A	Filaflex 95A	Filaflex 82A
Yield Strength	4.9E07 N/m^2	5.0E07 N/m^2	5.5E07 N/m^2	5.5E07 N/m^2
Tensile Strength	5.0E07 N/m^2	5.0E07 N/m^2	5.5E07 N/m^2	5.5E07 N/m^2
Elastic Modulus	3.5E09 N/m^2	1.5E08 N/m^2	6.0E07 N/m^2	2.6E07 N/m^2
Mass Density	1300 kg/m^3	1220 kg/m^3	1080 kg/m^3	1000 kg/m^3
Thermal expansion coefficient	8.5E-05 /Kelvin	1E-04 /Kelvin	-	-

D

Complementary Results

This appendix contains supplementary results of this study to complement those present in Chapter 5. First, it illustrates the load test that was performed to the entire prosthesis, to validate the pull test results of the small hand. Additionally, it complements Section 5.2.3 with the measured angulations of the device's movements and Section 5.2.2 with the results of the grasp type tests conducted on the larger hand. It also provides additional FEM analysis data, with the results of using Filaflex 82A and Filaflex 95A. Finally, it presents the final product characteristics, including costs, weigh and printing time.

D.1 Mechanical Tests

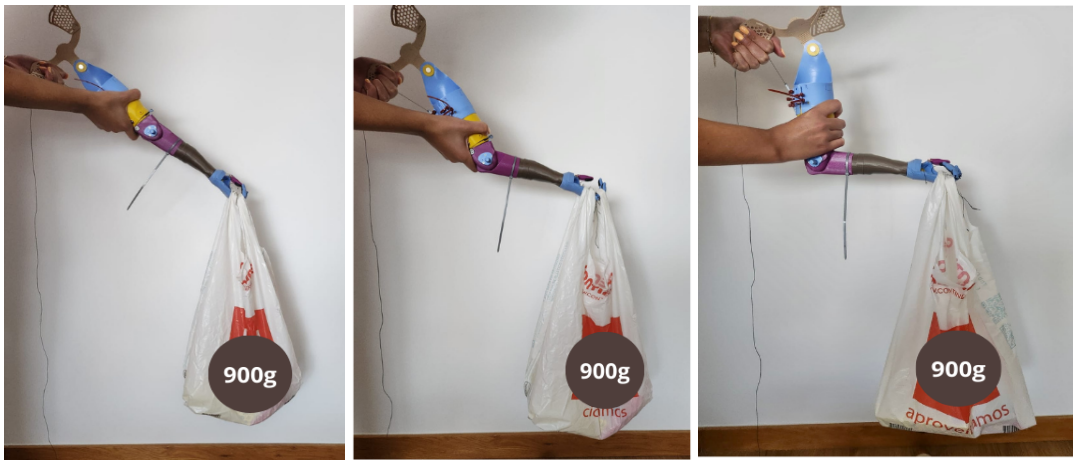

(a) Elbow position 1. (b) Elbow position 2. (c) Elbow position 3.

Figure D.1: Tensile test performed to the small prosthesis. Adapted from [55].

D.2 Goniometry

Table D.1: Measurements of prosthetic joint angles in degrees (± 0.5°).

	Measurements in Degrees (± 0.5°)						
	1	**2**	**3**	**4**	**5**	**Mean**	**SD**
Elbow Flexion							
Position 1	30.0	25.0	32.0	28.0	30.0	29.0	2.7
Position 2	70.0	72.0	74.0	73.0	69.0	71.6	2.1
Position 3	106.0	108.0	109.0	108.0	108.0	107.8	1.1
Shoulder Internal Rotation							
Position 1	0.0	2.0	1.0	2.0	3.0	0.0	1.1
Position 2	12.0	12.0	14.0	16.0	11.0	13.0	2.0
Position 3	29.0	28.0	26.0	24.0	25.0	26.4	2.1
Position 4	40.0	42.0	44.0	42.0	41.0	41.8	1.5
Position 5	52.0	52.0	54.0	52.0	53.0	52.6	0.9
Shoulder External Rotation							
Position 6	11.0	12.0	14.0	14.0	13.0	13.0	1.4
Position 7	22.0	22.0	24.0	25.0	23.0	23.2	1.3
Position 8	30.0	28.0	25.0	26.0	27.0	27.2	1.9
Radial Abduction							
Thumb	74.0	77.0	70.0	76.0	74.0	74.2	2.7
Palmar Abduction							
Thumb	44.0	48.0	47.0	43.0	50.0	46.4	2.9
Metacarpophalangeal Flexion							
Thumb	63.0	60.0	66.0	65.0	61.0	63.0	2.6
Index Finger	72.0	76.0	70.0	72.0	74.0	72.8	2.3
Middle Finger	80.0	76.0	78.0	79.0	78.0	78.2	1.5
Ring Finger	73.0	70.0	74.0	78.0	72.0	73.4	2.9
Little Finger	75.0	76.0	79.0	82.0	80.0	78.4	2.9
Proximal Interphalangeal Flexion							
Index	70.0	72.0	71.0	72.0	76.0	72.2	2.3
Middle Finger	82.0	86.0	83.0	83.0	85.0	83.8	1.6
Ring Finger	70.0	74.0	71.0	70.0	66.0	70.2	2.9
Little Finger	60.0	58.0	60.0	66.0	62.0	60.8	2.3
Distal Interphalangeal Flexion							
Index Finger	20.0	22.0	21.0	20.0	19.0	20.4	1.1
Middle Finger	18.0	19.0	20.0	18.0	20.0	19.0	1.0
Ring Finger	21.0	21.0	20.0	20.0	20.0	20.4	0.6
Little Finger	19.0	23.0	20.0	22.0	21.0	21.0	1.6
Interphalangeal Flexion							
Thumb	18.0	19.0	20.0	19.0	18.0	18.8	0.8

D.3 Grasp Type Tests

Table D.2: Results of the grasp type tests performed on the larger hand.

Grasp Classification	Grasp Type	Result
Power	Cylindrical Grasp (Large Diameter)	Yes (Up to 50 mm of diameter)
	Cylindrical Grasp (Small Diameter)	Yes (Up to 20 mm of diameter)
	Spherical Grasp	No
	Disk Grasp	Yes (Up to 60 mm of diameter and 15 mm of thickness)
Intermediate	Lateral Pinch	No
Precision	Tip Pinch	No
	Prismatic Finger	No
	Precision Disk	No
	Inferior Pincer	Yes (Limited to certain sizes and shapes)

D.4 Finite Element Analysis

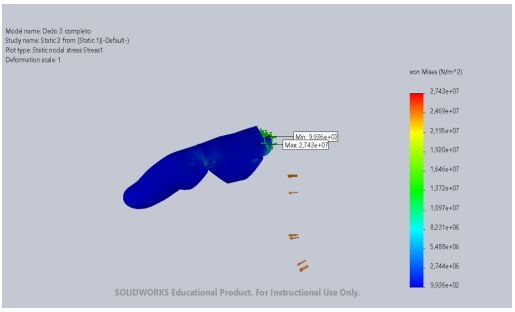

(a) Stress distribution.

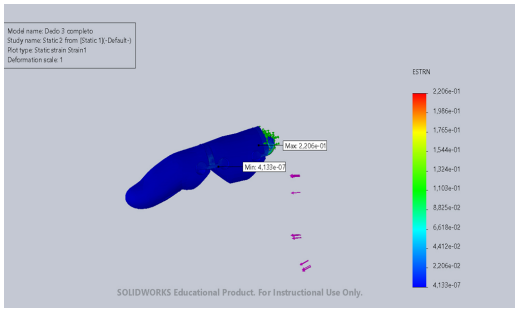

(b) Strain distribution.

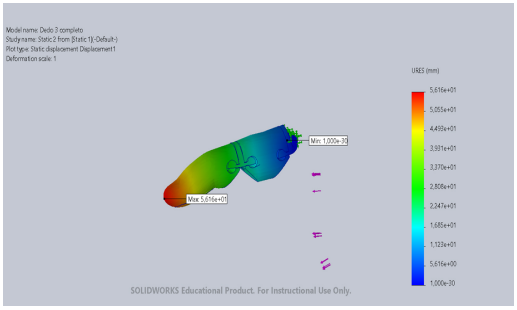

(c) Displacement distribution.

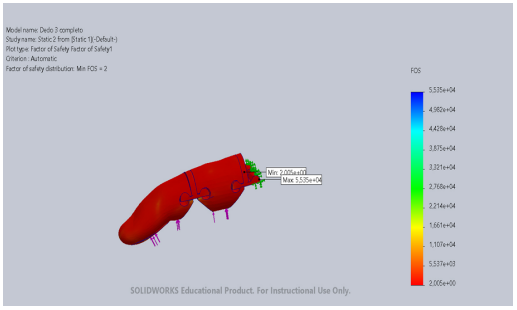

(d) Factor of safety distribution.

Figure D.2: Finite element analysis of the index finger with hinges made of Filaflex 95A.

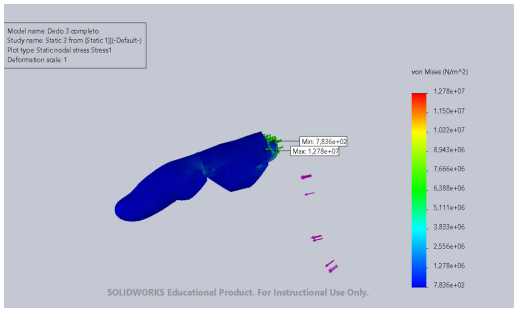

(a) Stress distribution.

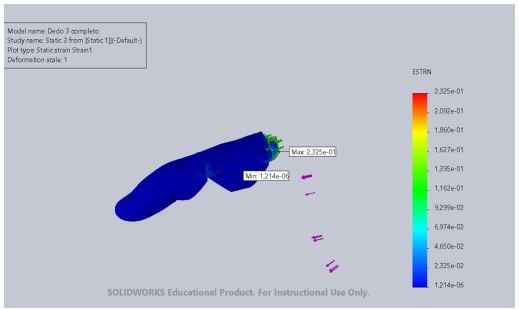

(b) Strain distribution.

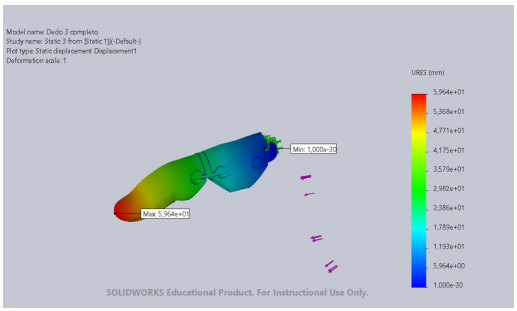

(c) Displacement distribution.

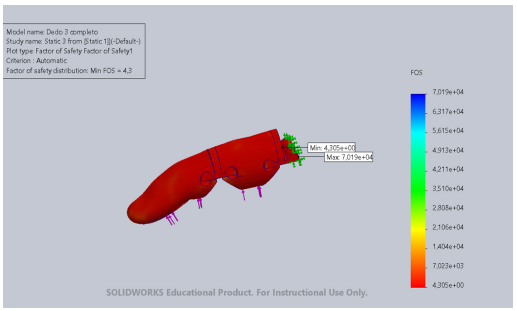

(d) Factor of safety distribution.

Figure D.3: Finite element analysis of the index finger with hinges made of Filaflex 82A.

D.5 Prosthesis Evaluation

Table D.3: Characteristics of the final prosthesis. Note: Using Filaflex 82A instead of TPU 98A would have similar results.

Characteristic	**PLA(21€/kg)**	**TPU 98A (29€/kg)**
Mass (g)	384.39	28
Cost (€)	8.07	1.63
Printing Time (h)	55h05	5h20

E

Drawings

This appendix includes the drawings of the "Puller and the "Cap", which belong to the "Elbow" region of the new prosthesis. It is important to note that the "Humeral medial", "Humeral lateral", "Humeral Central", "Shelbow lateral", "Shelbow medial" resulted from significant design modifications to the pre-existing parts. However, due to their organic shapes, these drawings are difficult to present with clarity.

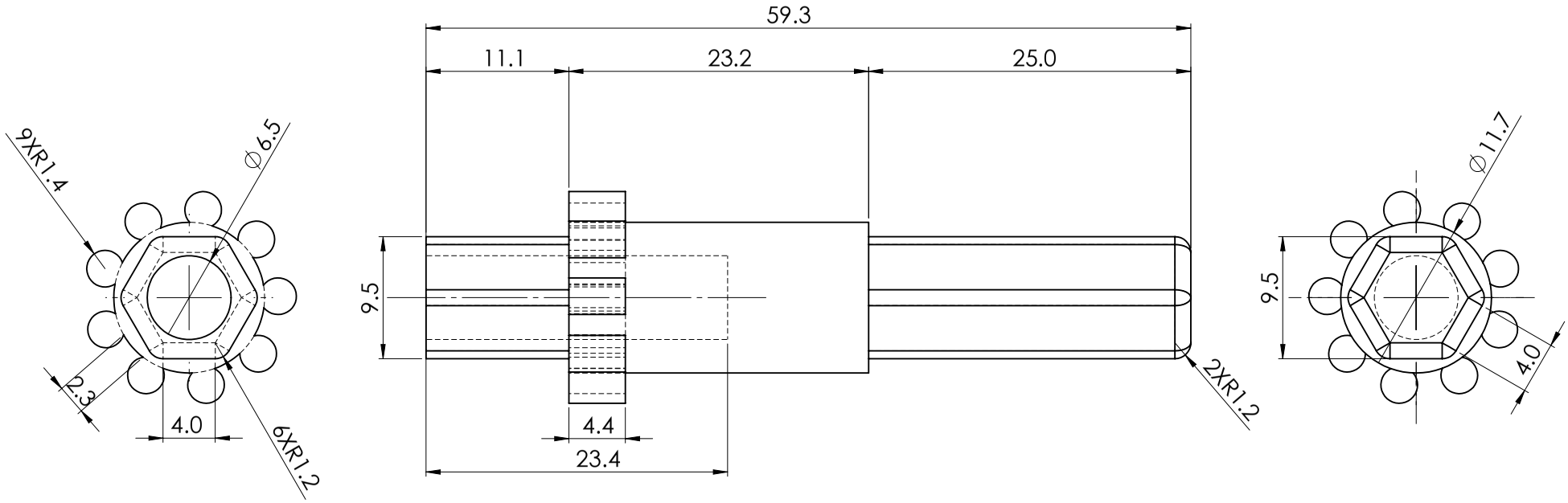

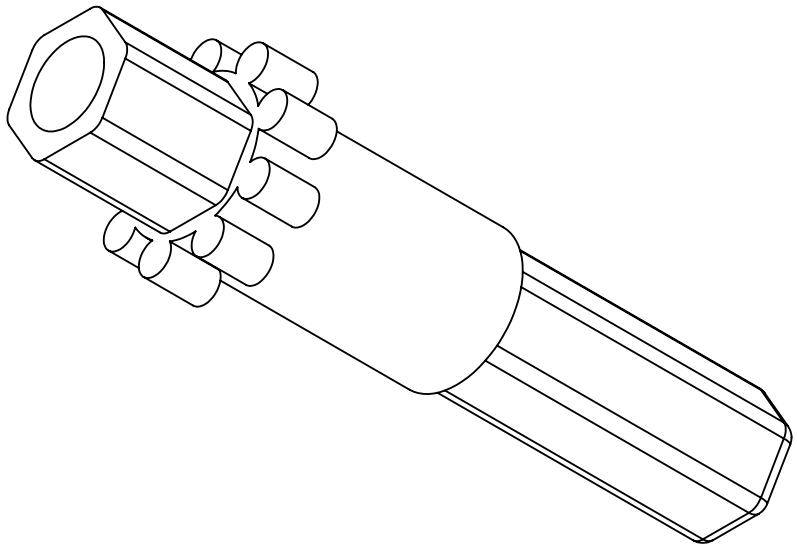

Proj.			NOVA SST	Inês Ludovino
Des. Copiou	08/24			
Visto				
3:1			Puller	Biomedical Engineering
Toleran. NP-265 Médio				

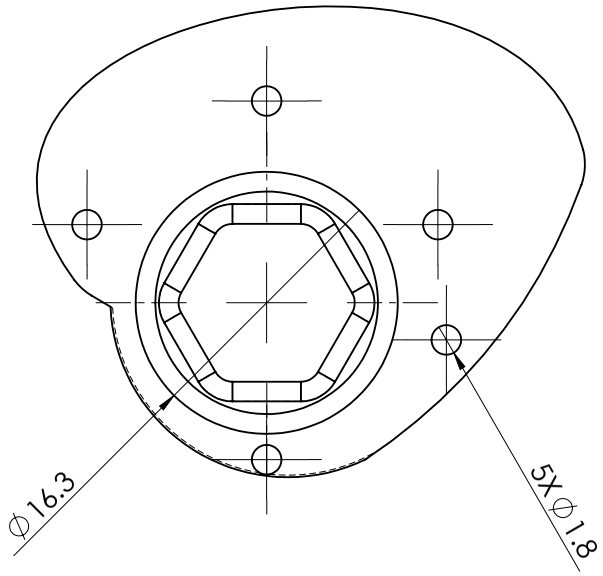

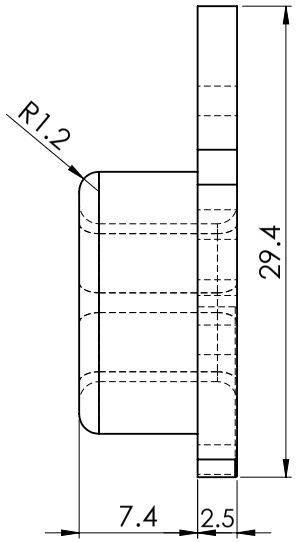

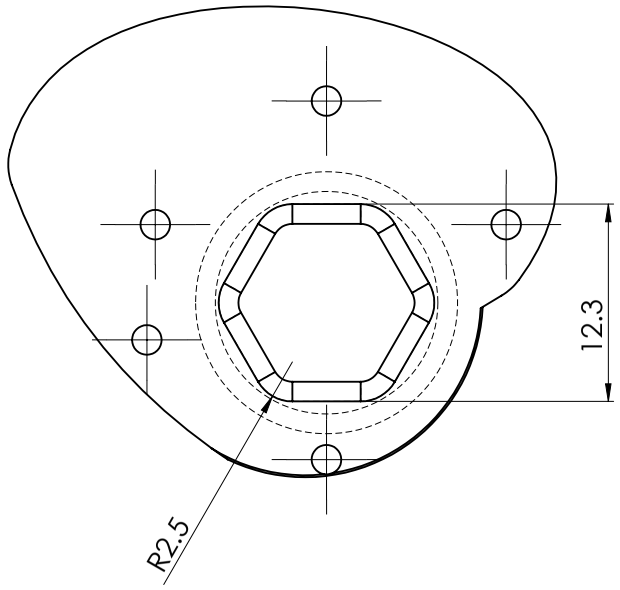

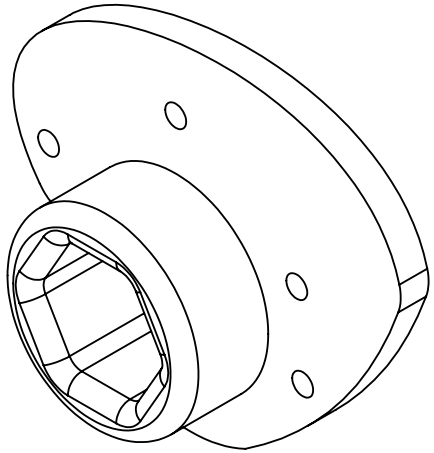

Proj.			NOVA SST	Inês Ludovino
Des. Copiou	08/24			
Visto				
3:1			Cap	Biomedical Engineering
Toleran. NP-265 Médio				

F

Prosthesis Assembly Guide

This appendix provides a comprehensive assembly guide of the developed prosthesis, offering step-by-step instructions accompanied by images. It also includes details on the tools, hardware, and other materials required for the assembly. The guide is organized into four sections - "Hand", "Forearm", "Elbow", "Shoulder" - each corresponding to a different region of the prosthesis. The assembly instructions are organized from distal to proximal, reflecting the order in which the design modifications were applied.

F.1 Hand

1. **Attach fingers to the palm**

   Required parts: 9 Hinges, 4 Phalanges, 5 Fingertips, Hand

   Required tools: pliers, sandpaper/file

   For the next instructions, follow the numbers notation represented in Figure F.1.

Figure F.1: Numbers notation.

- Trim the "Hinges" after printing with sandpaper or a file, to get smoother surfaces.
- Fit one side of the "Hinge" into the "Hand" as seen in Figure F.11a. Use pliers to stretch and fit the other side of the "Hinge". Repeat for "Hinges" numbers 1, 2, 4, 6 and 8.
- Insert one side of the "Hinge" into the finger "Phalanx" by hand, then use pliers to stretch and fit the other side as seen in Figure F.2b. Repeat for "Phalanges" 2, 4, 6 and 8.
- Insert the remaining "Hinges" 3, 5, 7 and 9 at the top of the finger "Phalanges".
- Attach each "Fingertip" to the corresponding "Hinge" as seen in Figure F.2c. Repeat for all five "Fingertips" 1, 3, 5, 7 and 9.

(a) Inserting Hinges. (b) Inserting Phalanges. (c) Inserting Fingertips.

Figure F.2: Assembly of the Hand.

2. **Whippletree mechanism**

   Required parts: Whippletree primary, Whippletree secondary

   Required tools and materials: polyester wire, nylon wire, scissors

   - Insert the polyester wires using a nylon wire as a guide if necessary, following the configuration shown in Figure F.3 and the steps below:
     - Insert one wire to connect the index finger, middle finger, and "Whippletree Primary," tying knots at the fingertip bars.
     - Insert a second wire to connect the ring finger, little finger, and "Whippletree Primary," also tying knots at the fingertip bars.
     - Insert a third wire to connect the thumb to the "Whippletree Secondary," tying a knot at the fingertip bar.

- Use another wire to connect the "Whippletree Primary" to the "Whippletree Secondary."

- Finally, attach the main wire to the "Whippletree Primary," ensuring it is long enough to reach the upper section of the device.

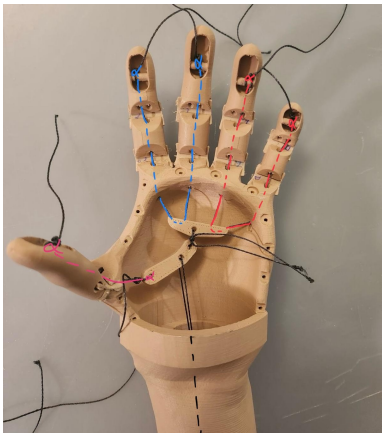

Figure F.3: Whippletree mechanism. Red line represents the wire through the pinky and the ring fingers. Blue line represents the wire through the index and the middle fingers. Pink line represents the wire through the thumb. Black line represents the main wire.

3. **Close the hand**

   Required parts: Palm cover, Finger grips

   Required hardware and tools: screws, screwdriver, pliers

   - Attach the "Palm cover" to the palm structure, by aligning it and putting the screws in place with a screwdriver.
   - Insert the finger "Grips" in the designated slots of the fingertips with the help of pliers.

Figure F.4: Palm cover and finger grips in position.

F.2 Forearm

Required parts: Forearm, Forearm base, Pin, Stopper
Required tools: screwdriver or similar tool

- Insert the "Pin" through the "Forearm" and the "Forearm base".

- Use a screwdriver or a similar tool to insert the "Stopper" from the "Hand"'s opening, along the forearm, and lock it into the "Pin".

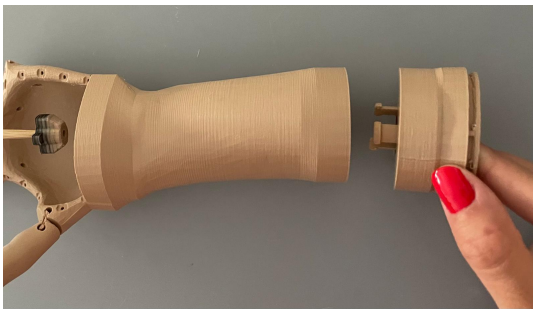

Figure F.5: Assembly of the Forearm.

F.3 Elbow

Required parts: Shelbow medial, Shelbow lateral (Shelbow parts), Humeral medial, Humeral lateral, Humeral central, Humeral core, Humeral latch pin (Humeral parts), Grip lock switch, Bottom plate, Top plate, Dowels, Puller and Cap

Required hardware and tools: Through bolt and nut, 8 screws, compression spring, oil and glue

1. **Shelbow region**

   - Insert the four "Dowels" into the "Shelbow medial" part.
   - Pass the wire trough the designated hole.
   - Position the "Shelbow medial" in the designated place on the forearm.
   - Close it with the "Shelbow lateral" part.
   - Insert the "Grip lock switch" into the "Shelbow medial" part.

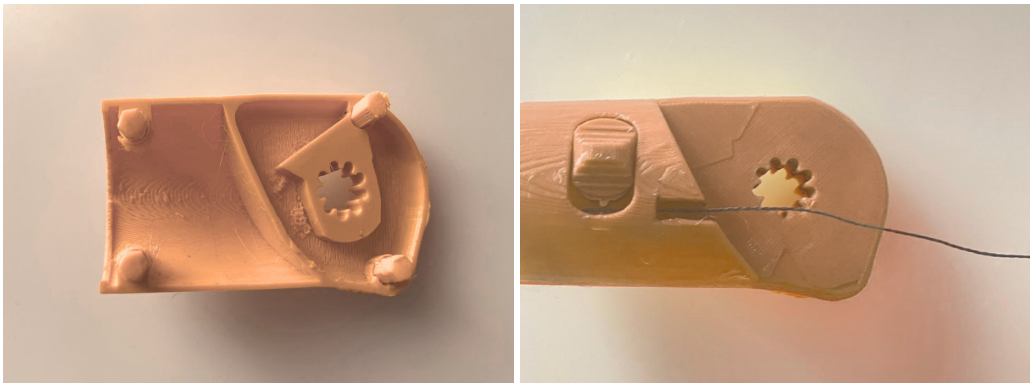

(a) "Dowels" in position. (b) Shelbow region assembled.

Figure F.6: Assembly of the Shelbow parts.

2. **Humeral region**

- Connect the 4 Humeral parts ("Humeral medial", "Humeral lateral", "Humeral central", "Humeral core") trough the bolt and its nut.
- Attach the "Bottom plate" using 4 screws, as in Figure F.7a.
- Insert the "Humeral latch pin", as in Figure F.7a.
- Attach the "Top plate" with 4 more screws, as in Figure F.7b.

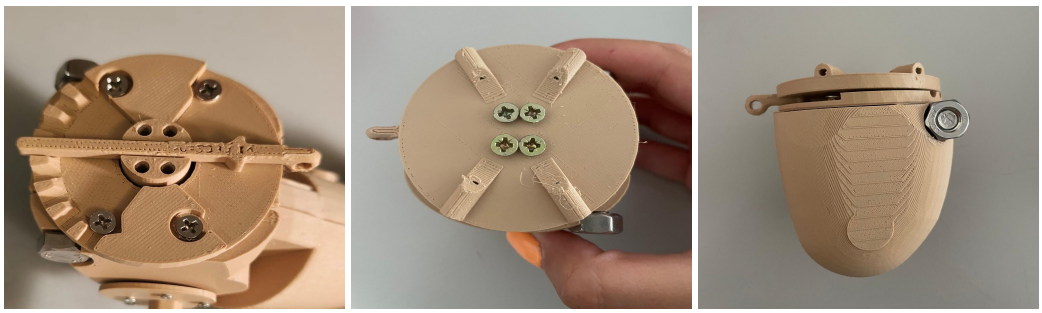

(a) "Bottom plate" and "Humeral latch pin" in place. (b) "Top plate" and screws in place. (c) Humeral region assembled.

Figure F.7: Assembly of the Humeral parts.

3. **Elbow flexion mechanism**

- Glue a compression spring at the "Puller"'s end and let it dry, as in Figure F.8a.
- Insert the "Puller" through the Humeral and Shelbow parts, followed by the "Cap" and the screws, as in Figure F.8b. It is recommended to use oil to lubricate the elbow flexion mechanism.

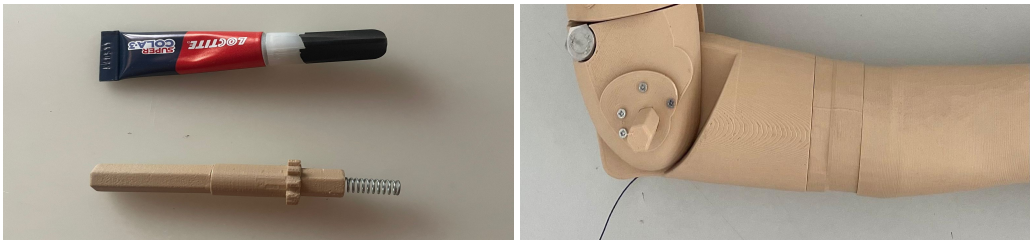

(a) Compression spring glued to the "Puller". (b) "Puller" and "Cap" inserted.

Figure F.8: Assembly of the Elbow.

F.4 Shoulder

Required parts: Upper arm base, Arm wrap, Shoulder joint cap, Shoulder joint core, Shoulder connector, Clavicle plate, Scapula plate

Required hardware, tools and material: screws, screwdriver, screws with caps, heat source, scissors, harness, cable revetement and clamps

1. **Thermoforming**

   - Using a heat source, such as a hairdryer, hot water steam or a heat gun, thermoform the "Arm wrap" and the "Shoulder connector". It is recommended to use the patient's shoulder and upper arm as molds for accuracy. If unavailable, use a printed mold or a similarly shaped object like a bottle or a cup.

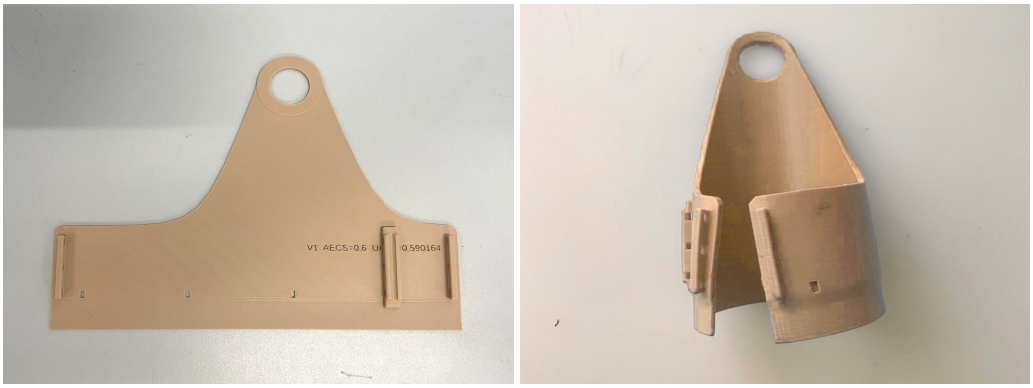

(a) "Arm wrap" before thermoforming. (b) "Arm wrap" after thermoforming.

Figure F.9: Thermoforming the "Arm Wrap".

(a) "Shoulder Connector" before thermoforming.

(b) "Shoulder Connector" after thermoforming.

Figure F.10: Thermoforming the "Shoulder Connector".

2. **Shoulder region**

   - Attach the "Upper arm base" to the "Top plate" with 4 screws.
   - Position the "Arm wrap" correctly and secure it with clamps.
   - Join the clavicle and scapula plates with the "Shoulder connector" using screws and their caps.
   - Connect the "Shoulder connector" to the "Arm wrap", "Cap joint" and "Cap core", with a screw and its cap.
   - Put the cable revetment in position and secure it with clamps.
   - Pass the wire trough the cable revetment and trough the "Scapula plate" corridor.
   - Tie a knot in the wire at the "Scapula plate" and trim any excess length.

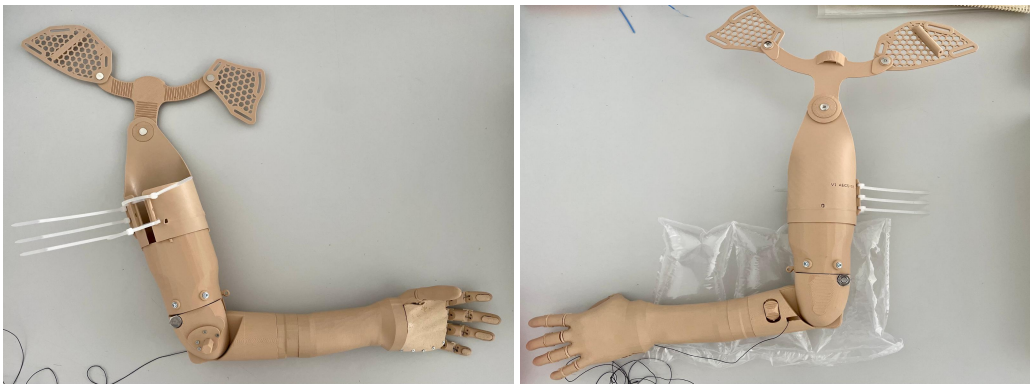

(a) Secure the "Arm wrap" with clamps.

(b) "Arm wrap" in position

Figure F.11: Assembly of the Shoulder.

3. **Harness**

   Required tools and materials: Velcro straps, glue and scissors

- With the prosthesis fitted on the amputee, pass the straps through the designated holes in the "Clavicle plate" and "Scapula plate," highlighted in red in the scheme shown in Figure F.12. Securely fasten the straps around the amputee's chest, following the configuration in the scheme. Use glue to secure the ends of the straps, and trim any excess material with scissors.

Figure F.12: Harness mechanism.